

# Noise Induced Universal Diffusive Transport in Fermionic Chains

Christopher M. Langlett<sup>1,\*</sup> and Shenglong Xu<sup>1</sup>

<sup>1</sup>*Department of Physics & Astronomy, Texas A&M University, College Station, Texas 77843, USA*

We develop a microscopic transport theory in a randomly driven fermionic model where the operator dynamics arise from the competition between noisy and static couplings. We map the noise-averaged operator equation of motion to a one-dimensional non-hermitian hopping model and solve it exactly. We uncover that universal diffusive behavior is attributed to an emergent noise induced bound state in the operator equations of motion at small momentum. As momentum increases, in the strong noise limit, the diffusive mode persists to  $k = 2\pi$  as the operator equation becomes the diffusion equation and is unaffected by additional arbitrarily strong static terms that commute with the local charge, including density-density interactions. On the other hand, at finite noise, the bound state enters a continuum of scattering states and vanishes. However, the bound state reemerges at an exceptional-like point in the spectrum after the bound-to-scattering state phase transition. We further characterize the fate of Stark localization in the presence of noise, where we ultimately show that noise washes away any signature of localization, and diffusion ensues.

An outstanding challenge of many-body physics is a complete explanation of how phenomenological laws governing irreversible macroscopic transport behavior emerge from reversible microscopic dynamics [1–3]. This challenge only magnifies in interacting quantum many-body systems, in both equilibrium and non-equilibrium processes [4, 5], by which, analytical results are difficult to achieve. Along these lines, one-dimensional systems [6, 7] are attractive because quantum fluctuations have a pronounced effect, leading to a wide array of quantum phenomena ranging from ballistic transport to localization. One appealing aspect of 1D is the existence of exact solutions to microscopic models [8, 9], such as the Heisenberg XXZ model [10], where spin transport revealed KPZ universality [11] at the isotropic point [12–17]. However, a complete characterization of quantum transport in solvable models remains challenging despite having access to the eigenenergies, excitations [9, 18–21].

Randomly driven models, in which couplings are random variables uncorrelated in time, are useful in understanding the spreading of a local operator under Heisenberg evolution known as the operator dynamics. Systems with added stochasticity reveal universal behavior after the noise washes away the microscopic details. These systems have had a reviving interest in the context of random Hamiltonians [22–27], noisy spin chains [28–34], dual unitary circuits [35, 36], replica disorder averaged random unitary circuits [37–39], and even paraxial optics [40]. In parallel, the rising unprecedented experimental control [41, 42] over isolated quantum many-body systems, such as superconducting qubits, offers the opportunity to probe one of the many faces of random unitary dynamics.

Despite tremendous progress, a complete characterization of the ingredients necessary for unorthodox transport to arise in interacting many-body systems is lacking. However, one approach is introducing a static term as a perturbation to access more generic information about late-time transport [30, 43]. A recent study [44] of a

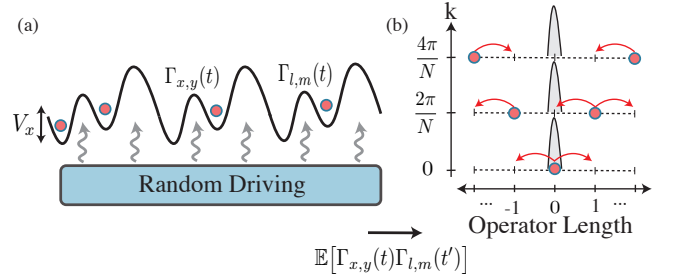


FIG. 1. *Noise Induced Non-Hermitian Hopping Model.* (a) Randomly driven non-interacting fermions in a spatially dependent potential,  $J_{x,x} = V_x$ . Classical noise  $\Gamma_{x,y}(t)$  models the random drive by couples locally to the hopping or density. (b) Noise-averaged operator equations of motion map onto a set of one-dimensional non-hermitian hopping models with a repulsive delta function. The  $x$ -axis is the operator length, and  $k$  is the center-of-mass momentum.

spin-1/2 chain with Brownian exchange couplings that fluctuate in space-time around a non-zero mean, revealed, through perturbation theory, late-time spin diffusion, albeit with a superdiffusive enhancement suggesting normal diffusion [45].

In this work, we develop a microscopic transport theory in a fermionic chain. The operator dynamics arise from the competition between randomly driven and arbitrarily strong static couplings. We analytically solve for the diffusion constant by mapping the noise-averaged operator equation of motion to a one-dimensional non-hermitian hopping model, which we compare to large-scale numerics. We uncover a diffusive mode that governs the late-time hydrodynamics at small  $k$ , attributed to an emergent non-perturbative bound state in the operator equations of motion. The diffusive mode persists in the strong noise limit as momentum increases to  $k = 2\pi$ . The operator equation becomes the diffusion equation and is unaffected by additional arbitrarily strong static terms that commute with the local charge, including density-density interactions.

The bound state enters a continuum of scattering states at finite noise and vanishes. However, the bound state reemerges at larger momentum at an exceptional-like point in the spectrum after the bound-to-scattering state phase transition. We further characterize the fate of Stark localization in the presence of noise, where we ultimately show that noise washes away any signature of localization, and diffusion ensues.

*Model.*— We explore the dynamics of one-dimensional non-interacting fermions with time-dependent noise, through the Hamiltonian,

$$H_t = \sum_{x,y} [J_{x,y} + \Gamma_{x,y}(t)] c_x^\dagger c_y, \quad (1)$$

where  $c_x^\dagger$  ( $c_x$ ) create (annihilate) an electron at site index  $x$ . The off diagonal elements of  $J_{x,y}$  and  $\Gamma_{x,y}(t)$  represent either static or driven hopping, while the diagonal elements represent a static or driven potential. The amplitudes  $\{\Gamma_{x,y}\}$  are drawn independently for each pair of sites  $(x,y)$  from a Gaussian distribution with zero mean and variance,

$$\mathbb{E}[\Gamma_{x,y}(t)\Gamma_{l,m}(t')] = \Gamma_{xy}\delta_{x,l}\delta_{y,m}\delta(t-t'). \quad (2)$$

Where  $\mathbb{E}[\cdot]$  denotes the average over disorder,  $\Gamma_{x,y}$  sets the energy scale of the system, and  $\delta(t-t')$  implies the couplings are correlated at a single instance in time. We study the time-dependent correlation functions analytically and numerically, to reveal the long-distance late-time hydrodynamic transport in the presence of noise. In the Heisenberg picture, the infinitesimal operator evolves stochastically,  $\mathcal{O}_{t+dt} = e^{iH_t dt} \mathcal{O}_t e^{-iH_t dt}$ . The evolution equation for a generic noise-averaged operator follows from expanding the flow of  $\mathcal{O}_t$  up to second-order in  $dt$  and averaging the noise,

$$d\bar{\mathcal{O}}_t = \sum_{x,y} \left[ iJ_{x,y} [c_x^\dagger c_y, \bar{\mathcal{O}}_t] + \Gamma_{x,y} \mathcal{L}_{x,y} [\bar{\mathcal{O}}_t] \right] dt. \quad (3)$$

Here the average dynamics are governed by an effective Lindblad description where  $\mathcal{L}_{x,y}[\ast] = L_{x,y}^\dagger \ast L_{x,y} - \frac{1}{2}\{L_{x,y}^\dagger L_{x,y}, \ast\}$  with  $L_{x,y} = c_x^\dagger c_y + h.c.$ , and  $\{\cdot, \cdot\}$  standing for the anti-commutator. Competition between coherent and incoherent dynamics drive the time evolved noise-averaged operator in the late-time limit to the steady state  $\lim_{t \rightarrow \infty} \bar{\mathcal{O}}_t = \sum_x n_x$  from charge conservation.

*Characterizing Transport.*— Universal behavior of the random unitary dynamics is ascertained through the infinite-temperature fermion density-density correlation function,

$$C_{x,y}(t) = \frac{1}{2^N} \text{tr} \left[ \left( n_x(t) - \frac{1}{2} \right) \left( n_y - \frac{1}{2} \right) \right], \quad (4)$$

where  $n_x(t)$  denotes the time-evolved density operator at site index  $x$  in the Heisenberg picture. The density-

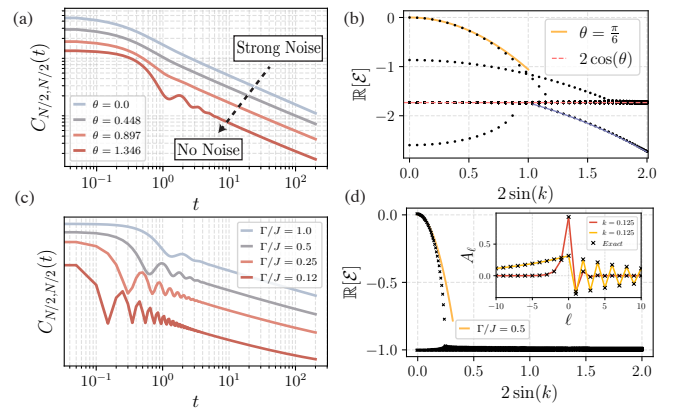


FIG. 2. *Operator dynamics and Bound State Coefficients.* (a) Noisy-hopping operator dynamics. (b) Real part of the eigenvalue spectrum of Eq. (3), at small  $k$  the largest real eigenvalue is given by the diffusive mode which corresponds to Eq. (16) [yellow curve]. The red curve is the scattering state continuum, and the blue curve indicates a double degeneracy after crossing the exceptional-like point. (c) Operator dynamics for the noisy potential and static hopping. The oscillations arise from the bound-to-scattering state phase transition. (d) Real part eigenvalue spectrum for the noisy potential, where there is a single bound state corresponding to the diffusive mode with energy given by Eq. (13). Inset: The coefficients  $A_\ell$  from Eq. (12) for different  $k$  compared to diagonalizing of Eq. (11). Simulation parameters: (a) and (c)  $N = 400$ ,  $dt = 0.05$ ,  $\ell_{\max} = N/2$ . (b) and (d)  $N = 4000$ ,  $\Gamma/J = 1$ . The dynamics curves are offset for clarity.

density correlation function Eq. (4) decays with an algebraic tail at late times,

$$\lim_{t \rightarrow \infty} \lim_{N \rightarrow \infty} C_{N/2, N/2}(t) \sim t^{-1/z}. \quad (5)$$

The dynamical exponent  $z$  classifies the universal hydrodynamic transport behavior, for example,  $z = 1$  for ballistic,  $1 < z < 2$  for superdiffusive,  $z = 2$  for diffusive,  $z > 2$  is subdiffusive, and  $z = \infty$  for localized.

*Operator Dynamics.*— In the absence of interactions, the support of the Heisenberg operator  $n_x(t)$  is constant under evolution, permitting the expansion,

$$n_x(t) = \sum_{m,n=1}^N A_{m,n}(t) c_m^\dagger c_n. \quad (6)$$

With the initial condition,  $A_{m,n}(0) = \delta_{m,x} \delta_{n,x}$ . However, working in a different set of coordinates  $\ell = n - m$  and  $\mathcal{R} = n + m$  representing the operator length and center-of-mass is more convenient. In all examples, the noise-averaged operator equation is translation invariant in  $\mathcal{R}$ . A Fourier transformation maps Eq. (3) to equations for  $A_{\ell,k}$  describing a one-dimensional hopping model on a fictitious lattice of operator length  $\ell$  with the center of mass momentum  $k$ . The correlation function is given by,  $\frac{1}{8\pi} \int dk A_{0,k}(t) e^{ik(x-y)}$ , where  $A_{\ell,k}(t)$  is the time-evolved

wavefunction of the effective hopping model and  $A_{l,k} = \delta_{l,0}$  at  $t = 0$ . At finite noise, the effective model is non-Hermitian, and the slowest decaying mode controls the transport.

There are two well-studied limits of Eq. (3); no noise and strong noise. The former limit is with  $\Gamma_{x,y} = 0$  and static nearest-neighbor hopping ( $J_{x,x} = 0$ ,  $J_{x,x+1} = J$ ). The averaged operator equation becomes,

$$\partial_t A_{\ell,k} = t_k [A_{\ell+1,k} - A_{\ell-1,k}], \quad t_k = 2J \sin(k). \quad (7)$$

Here  $t_k$  is the effective hopping strength, leading to the correlation function,

$$C_{x,y}(t) = \frac{1}{4} \mathcal{J}_{x-y}^2(2t). \quad (8)$$

Here  $\mathcal{J}_{x-y}(2t)$  is the Bessel function of the first kind of order  $x-y$  with  $J = 1$ . The late-time behavior of the correlation function,  $\lim_{t \rightarrow \infty} C_{N/2, N/2}(t) = 1/\pi t$ , indicating an exponent  $z = 1.0$ .

*Strongly Driven Hopping.*— We now consider strongly driven hopping with  $J_{x,y} = 0$  and  $\Gamma_{x,y} = \delta_{|x-y|,1}$  in Eq. (3). In this limit, the operator length  $\ell = 0$ , which characterizes the correlation function Eq. (4) is decoupled from all other operator lengths, leading to the diffusion equation,

$$\partial_t A_{0,\mathcal{R}} = -2A_{0,\mathcal{R}} + A_{0,\mathcal{R}+2} + A_{0,\mathcal{R}-2}. \quad (9)$$

Moreover, the correlation function becomes,

$$C_{x,y}(t) = \frac{1}{4} e^{-2t} \mathcal{I}_{x-y}(2t). \quad (10)$$

Here  $\mathcal{I}_{x-y}(2t)$  is the modified Bessel function of the first kind of order  $x-y$ . The asymptotic scaling of Eq. (10) is,  $\lim_{t \rightarrow \infty} C_{N/2, N/2}(t) = 1/2\sqrt{t\pi}$  corresponding to the exponent  $z = 2$ . Including a static potential ( $J_{x,x} = V_x$ ) that couples to the density do not affect the late time behavior because it commutes with the local charge  $n_x$  and the noisy hopping term leaves  $n_x$  unchanged. More generally, including any static term that commutes with the local charge, even the density-density interaction,  $n_x n_y$ , will not affect the diffusive hydrodynamic mode in Eq. (9), rendering the same correlation function and diffusion transport.

*Noisy Potential and Static Hopping.*— As our next example, we consider a strongly driven potential where the density is time dependent rather than the hopping. Specifically, in Eq. (3) we have that  $\Gamma_{x,y} = \Gamma \delta_{x,y}$ , and  $J_{x,y} = J \delta_{|x-y|,1}$ . The operator equation of motion becomes,

$$\begin{aligned} \partial_t A_{0,k} &= t_k [A_{1,k} - A_{-1,k}] \\ \partial_t A_{\ell,k} &= t_k [A_{\ell+1,k} - A_{\ell-1,k}] - \Gamma A_{\ell,k}. \end{aligned} \quad (11)$$

The second equation describes the bulk dynamics with  $\ell > 0$  and  $\ell < 0$  [46]. The second equation connects

the bulk dynamics by specifying the boundary condition  $\ell = 0$ . The equations describe a 1D hopping model on a fictitious lattice defined by the operator length  $\ell$  with an imaginary potential at  $\ell = 0$ ; similar to the standard Schrödinger equation with a  $\delta$  potential, both scattering and bound states exist in the spectrum. The bulk equation fixes the real part of the eigenvalue of scattering states to be  $-\Gamma$ . Because the model is non-hermitian, the non-positive real parts of the eigenvalues of the above matrix always drive the system to a steady state in the late-time limit, corresponding to the eigenvalue with the maximal real part, namely, the eigenstate decays slowest during time evolution. In the long wavelength limit, we now illustrate a bound state centered at  $\ell = 0$  with real eigenvalue scaling as  $-k^2$  dominates the dynamics.

The bulk equation in Eq. (11) is translation invariant in  $\mathcal{R}$  and solved with the bound state ansatz,

$$A_{\ell,k} = \begin{cases} A e^{q\ell} & \text{if } \ell \leq 0 \\ A e^{-q\ell + i\pi\ell} & \text{if } \ell \geq 0. \end{cases} \quad (12)$$

Here  $A$  is an overall normalization. Inserting the above solution into the bulk equation, we find that  $\mathcal{E}_q = 4J \sin(k) \sinh(q) - \Gamma$  where the allowed values of  $q$  is determined by the boundary condition. We find  $q = \text{arccosh}[\Gamma/4J \sin(k)]$ , giving the bound state energy in the low momentum limit,

$$\mathcal{E}_q = \sqrt{\Gamma^2 - 16J^2 \sin^2(k)} - \Gamma \approx -\frac{8J^2 k^2}{\Gamma}. \quad (13)$$

Regardless of the strength of the noisy-driven potential, a bound state exists at small  $k$  with energy  $\mathcal{E}_q \sim k^2$ , leading to a long-time diffusive tail.

As  $k$  increases,  $q$  decreases, becoming zero at a critical  $k$  given by  $4J \sin k = \Gamma$  for  $\Gamma < 4J$ , at which the energy equals  $-\Gamma$  and the bound state enters the continuum of scattering states and vanishes [see Fig. 2(d)]. This transition manifests in the long-time behavior of the time-dependent correlation function by displaying increased oscillations before crossing over to diffusion; see Fig. 2(c) for numerical simulations of Eq. (3) for different  $\Gamma/J$ . In the inset of Fig. 2(d), we compare our analytical result for  $A_\ell$  to diagonalization of the eigenvalue equations, when  $k = 0.252$ ,  $q \approx 0$  and increasing  $k$  anymore cause the solution to crossover to a scattering state.

*Finite-Noise Hopping.*— We now consider transport at finite noise where there is time dependent and static nearest neighbor hopping such that  $\Gamma_{x,x+1} = \cos(\theta)$  and  $J_{x,x+1} = \sin(\theta)$ . For  $\theta = \pi/2$  we recover the free fermion limit, while  $\theta = 0$  recovers the strong drive limit. In this instance, we break the eigenvalue equations into the following bulk and boundary equations,

$$\begin{aligned} \mathcal{E}_q A_0 &= t_k(\theta) [A_1 - A_{-1}] - 4 \cos(\theta) \sin^2(k) A_0 \\ \mathcal{E}_q A_{\pm 1} &= \pm t_k(\theta) [A_{\pm 2} - A_0] + \cos(\theta) [A_{\mp 1} - 2A_{\pm 1}] \\ \mathcal{E}_q A_\ell &= t_k(\theta) [A_{\ell+1} - A_{\ell-1}] - 2 \cos(\theta) A_\ell. \end{aligned} \quad (14)$$

Here  $t_k(\theta) = 2 \sin(\theta) \sin(k)$  is the hopping strength of the non-hermitian model,  $|\ell| > 1$ . The first three equations are the boundary conditions, and the third describes the bulk, which fixes the real part of the scattering state energy to be  $-2 \cos(\theta)$ . The ansatz that decays on both sides of  $\ell = 0$  similar to Eq. (12) determines the bound state. Inserting into the eigenvalue equation gives the energy  $\mathcal{E}_q = 2t_k(\theta) \sinh(q) - 2 \cos(\theta)$  where  $q$  is constrained by,

$$\left[ \mathcal{E}_q + 4 \sin^2(k) \cos(\theta) \right] \left[ e^q + \frac{\cot(\theta)}{2 \sin(k)} \right] = -2t_k(\theta) \quad (15)$$

The above equation is an exactly solvable cubic equation, which at small  $k$  admits two physical solutions, one that begins at  $\mathcal{E}_q = 0$  [see yellow curve in Fig. 2(b)] and the other at  $\mathcal{E}_q = -3 \cos(\theta)$  [see lowest branch in Fig. 2(b)] and are the eigenvalues with the largest (smallest) real part. The branch in Fig. 2(b) beginning at  $\mathcal{E}_q = -\cos(\theta)$  is determined by solving Eq. (14) assuming  $A_0 = 0$ . Moreover, the bound state energy is given by,

$$\mathcal{E}_q = -\frac{2}{3} \left[ (5 + \cos(2\theta)) \sec(\theta) \right] k^2. \quad (16)$$

Regardless of the strength of the noisy-driven hopping, a diffusive mode always exists at small momentum visualized by the yellow curve in Fig. 2(b). We substantiate this result with numerical simulations of Eq. (3) for different  $\theta$  in Fig. 2(a) where the late-time tail is fitted with an exponent  $z = 2$ . However, as momentum increases the two real energies of Eq. (15) coalesce at a point similar to an exceptional point [47, 48] where the solutions become a conjugate pair of complex energies visualized by the doubly degenerate points in Fig. 2(b) indicated with a blue curve. Just as in the noisy-potential there is a scattering state transition, which occurs when the diffusive mode crosses the line at  $-2 \cos(\theta)$ , see Fig. 2(b).

*Stark Linear Potential.*— The system exhibited ballistic transport in the clean limit in the previous examples. However, no matter how weak, any external noise caused the transport to become diffusive in the long-time limit. Now, we will turn our attention to the opposite limit, where in the clean limit, the system undergoes localization and investigate its behavior in the presence of noise. We will study Wannier-Stark localization in the presence of noise [49, 50]. Specifically, we consider the static linear potential  $J_{x,x} = -\gamma x$  in addition to the noisy hopping. Here  $\gamma$  is the slope of the potential [see Fig. 3(a)]. Remarkably, despite a spatially inhomogeneous linear potential, the operator equation remains translation invariant in  $\mathcal{R}$  and can be labeled by momentum  $k$ . The bulk eigenvalue equation for finite noise becomes,

$$\begin{aligned} \mathcal{E}_q A_{\ell,k} \\ = t_k(\theta) [A_{\ell+1,k} - A_{\ell-1,k}] + [i\gamma\ell - 2 \cos(\theta)] A_{\ell,k} \end{aligned} \quad (17)$$

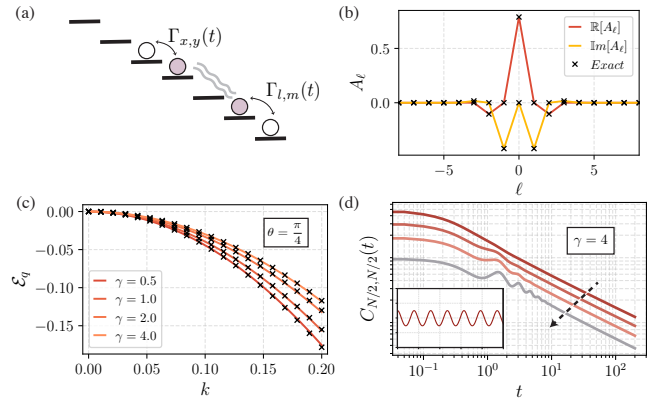


FIG. 3. *Noisy Linear Potential.* (a) Caricature of noise driven free fermions in a linear potential. (b) We plot the real and imaginary part of an eigenstate in the Stark localized phase from Eq. (17) compared to exact diagonalization with  $\gamma = 4$ , and hopping strength  $t_k(\theta) = 1.17$ . (c) Bound state energy as a function of momentum  $k$  with  $\theta = \pi/4$  for different  $\gamma$  compared to exact diagonalization of Eq. (17) [black crosses]. (d) Operator dynamics for different noise strengths. Inset: Bloch oscillations from localization ( $\theta = \pi/2$ ) in the absence of noise. Parameters: (b) and (c)  $N = 8000$ ,  $\ell_{\max} = N/2$  and (d)  $N = 400$ ,  $dt = 0.05$ ,  $\ell_{\max} = N/2$ ,  $\gamma = 4$ ,  $\theta = [0.445, 0.897, 1.12, 1.34]$ . The dynamics curves are offset for clarity.

The effective picture now is a one-dimensional non-hermitian hopping model in an imaginary linear potential. The bulk operator equation is no longer translation invariant in  $\ell$ , which permitted the plane wave ansatz Eq. (12). Here by solving the bulk recursion relation,  $A_\ell$  instead takes the form,

$$A_{\ell,k} = \begin{cases} A\mathcal{I}_{\nu_-}(-2it_k(\theta)/\gamma) & \text{if } \ell < -1 \\ B\mathcal{I}_{\nu_+}(-2it_k(\theta)/\gamma) & \text{if } \ell > 1. \end{cases} \quad (18)$$

where  $\nu_\pm = i(\mathcal{E}_q + 2 \cos(\theta))/\gamma \pm \ell$ . For  $\theta = \pi/2$  the operator equations are anti-hermitian leading to an equally spaced tower of purely imaginary eigenvalues,  $\mathcal{E}_q(\pi/2) = i\gamma q$  for  $q \in \{-\ell_{\max}, \ell_{\max}\}$  which is independent of the momentum  $k$ . The corresponding unnormalized eigenstates are  $A_{\ell,k} = \mathcal{I}_{\ell-q}(-4i \sin(k)/\gamma)$  [see Fig. 3(b)] which are Wannier-Stark localized [51–54] and no transport occurs. Finite noise renders the operator equations non-hermitian, causing an eigenvalue to become purely real, which is the long wavelength mode. Substituting the bulk ansatz into the boundary condition, we find in the small  $k$  limit the bound state energy is,

$$\mathcal{E}_q = -2 \cos(\theta) \left[ \frac{5 + 2\gamma^2 + \cos(2\theta)}{\gamma^2 + 3 \cos^2(\theta)} \right] k^2. \quad (19)$$

which is diffusive, similar to Anderson localized models with global noise [30, 55, 56], but different from other noise models [57, 58]. We emphasize that when  $\gamma = 0$ , Eq. (16) is recovered. In Fig. 3(c) we compare Eq. (19) to

diagonalizing the operator equations Eq. (3) for different potential strengths. For the Stark localized case  $\theta = \pi/2$  the energy vanishes because there is no longer a bound state with a purely real energy but rather a spectrum of bound states discussed above. Interestingly, as  $\gamma \rightarrow \infty$ , the diffusion constant remains finite and controlled by the noise strength since  $\mathcal{E}_q \rightarrow -4 \cos(\theta)k^2$ , indicating that stark location is unstable against external noise. We simulate the operator dynamics of Eq. (17) for different noise strengths with  $\gamma = 4$  where we find diffusion except identically at the point  $\theta = \pi/2$  where Bloch oscillations are present.

*Conclusion.*— Through a combination of analytics and large-scale numerics, this work developed a transport model where the operator dynamics arise from the competition between randomly driven and static couplings. We exactly solve for the diffusion constant by determining the emergent bound state of an effective one-dimensional non-hermitian hopping model at small momentum. For strongly driven hopping, the noise-averaged equation satisfies the diffusion equation, which is robust to arbitrarily strong static terms that commute with the local charge, including interactions. As momentum increases, the bound state enters a continuum of scattering states and vanishes. Surprisingly, at momentum beyond the bound-to-scattering state phase transition, the bound state reemerges at an exceptional-like point. We further find Stark localization cannot overcome the diffusive mode from noise. Future work could be understanding transport when the model has long-range hopping or correlating the noise [59].

*Acknowledgement.*— We thank Lakshya Agarwal and Joaquin F. Rodriguez-Nieva for useful discussions. The numerical simulations in this work were conducted with the advanced computing resources provided by Texas A&M High Performance Research Computing.

---

\* clanglett85@tamu.edu

- [1] L. D’Alessio, Y. Kafri, A. Polkovnikov, and M. Rigol, From quantum chaos and eigenstate thermalization to statistical mechanics and thermodynamics, *Advances in Physics* **65**, 239 (2016).
- [2] M. Srednicki, Chaos and quantum thermalization, *Phys. Rev. E* **50**, 888 (1994).
- [3] J. M. Deutsch, Quantum statistical mechanics in a closed system, *Phys. Rev. A* **43**, 2046 (1991).
- [4] A. Polkovnikov, K. Sengupta, A. Silva, and M. Vengalattore, Colloquium: Nonequilibrium dynamics of closed interacting quantum systems, *Rev. Mod. Phys.* **83**, 863 (2011).
- [5] J. Eisert, M. Friesdorf, and C. Gogolin, Quantum many-body systems out of equilibrium, *Nature Physics* **11**, 124 (2015).
- [6] T. Giamarchi, *Quantum physics in one dimension*, Vol. 121 (Clarendon press, 2003).
- [7] X.-W. Guan, M. T. Batchelor, and C. Lee, Fermi gases in one dimension: From bethe ansatz to experiments, *Rev. Mod. Phys.* **85**, 1633 (2013).
- [8] H. Bethe, Zur theorie der metalle: I. eigenwerte und eigenfunktionen der linearen atomkette, *Zeitschrift für Physik* **71**, 205 (1931).
- [9] F. H. Essler, H. Frahm, F. Göhmann, A. Klümper, and V. E. Korepin, *The one-dimensional Hubbard model* (Cambridge University Press, 2005).
- [10] M. Takahashi, Thermodynamics of one-dimensional solvable models, *Thermodynamics of One-Dimensional Solvable Models* (2005).
- [11] M. Kardar, G. Parisi, and Y.-C. Zhang, Dynamic scaling of growing interfaces, *Phys. Rev. Lett.* **56**, 889 (1986).
- [12] M. Ljubotina, M. Žnidarič, and T. c. v. Prosen, Kardar-parisi-zhang physics in the quantum heisenberg magnet, *Phys. Rev. Lett.* **122**, 210602 (2019).
- [13] M. Ljubotina, M. Žnidarič, and T. Prosen, Spin diffusion from an inhomogeneous quench in an integrable system, *Nature communications* **8**, 16117 (2017).
- [14] H. Spohn, The 1+1 dimensional kardar–parisi–zhang equation: more surprises, *Journal of Statistical Mechanics: Theory and Experiment* **2020**, 044001 (2020).
- [15] F. Weiner, P. Schmitteckert, S. Bera, and F. Evers, High-temperature spin dynamics in the heisenberg chain: Magnon propagation and emerging kardar-parisi-zhang scaling in the zero-magnetization limit, *Phys. Rev. B* **101**, 045115 (2020).
- [16] A. Scheie, N. Sherman, M. Dupont, S. Nagler, M. Stone, G. Granroth, J. Moore, and D. Tennant, Detection of kardar–parisi–zhang hydrodynamics in a quantum heisenberg spin-1/2 chain, *Nature Physics* **17**, 726 (2021).
- [17] D. Wei, A. Rubio-Abadal, B. Ye, F. Machado, J. Kemp, K. Srakaew, S. Hollerith, J. Rui, S. Gopalakrishnan, N. Y. Yao, *et al.*, Quantum gas microscopy of kardar-parisi-zhang superdiffusion, *Science* **376**, 716 (2022).
- [18] M. Gaudin, Thermodynamics of the heisenberg-ising ring for  $\Delta > 1$ , *Phys. Rev. Lett.* **26**, 1301 (1971).
- [19] J.-S. Caux and J. M. Maillet, Computation of dynamical correlation functions of heisenberg chains in a magnetic field, *Phys. Rev. Lett.* **95**, 077201 (2005).
- [20] A. Klauser, J. Mossel, J.-S. Caux, and J. van den Brink, Spin-exchange dynamical structure factor of the  $s = 1/2$  heisenberg chain, *Phys. Rev. Lett.* **106**, 157205 (2011).
- [21] A. Klümper, Integrability of quantum chains: theory and applications to the spin-1/2 xxx chain, *Quantum magnetism*, 349 (2008).
- [22] S. H. Shenker and D. Stanford, Stringy effects in scrambling, *Journal of High Energy Physics* **2015**, 1 (2015).
- [23] N. Lashkari, D. Stanford, M. Hastings, T. Osborne, and P. Hayden, Towards the fast scrambling conjecture, *Journal of High Energy Physics* **2013**, 1 (2013).
- [24] S. Xu and B. Swingle, Locality, quantum fluctuations, and scrambling, *Phys. Rev. X* **9**, 031048 (2019).
- [25] P. Saad, S. H. Shenker, and D. Stanford, A semiclassical ramp in syk and in gravity, *arXiv preprint arXiv:1806.06840* (2018).
- [26] T. Zhou and X. Chen, Operator dynamics in a brownian quantum circuit, *Phys. Rev. E* **99**, 052212 (2019).
- [27] C. Sünderhauf, L. Piroli, X.-L. Qi, N. Schuch, and J. I. Cirac, Quantum chaos in the brownian syk model with large finite n: Otcos and tripartite information, *Journal of High Energy Physics* **2019**, 1 (2019).
- [28] M. Knap, Entanglement production and information

- scrambling in a noisy spin system, *Phys. Rev. B* **98**, 184416 (2018).
- [29] D. A. Rowlands and A. Lamacraft, Noisy coupled qubits: Operator spreading and the fredrickson-andersen model, *Phys. Rev. B* **98**, 195125 (2018).
- [30] S. Gopalakrishnan, K. R. Islam, and M. Knap, Noise-induced subdiffusion in strongly localized quantum systems, *Phys. Rev. Lett.* **119**, 046601 (2017).
- [31] M. Singh and S. Gangadharaiah, Driven quantum spin chain in the presence of noise: Anti-kibble-zurek behavior, *Phys. Rev. B* **104**, 064313 (2021).
- [32] T. Swann, D. Bernard, and A. Nahum, Spacetime picture for entanglement generation in noisy fermion chains, *arXiv preprint arXiv:2302.12212* (2023).
- [33] M. Fava, L. Piroli, T. Swann, D. Bernard, and A. Nahum, Nonlinear sigma models for monitored dynamics of free fermions, *arXiv preprint arXiv:2302.12820* (2023).
- [34] T. Jin, A. Krajenbrink, and D. Bernard, From stochastic spin chains to quantum kardar-parisi-zhang dynamics, *Phys. Rev. Lett.* **125**, 040603 (2020).
- [35] L. Piroli, B. Bertini, J. I. Cirac, and T. c. v. Prosen, Exact dynamics in dual-unitary quantum circuits, *Phys. Rev. B* **101**, 094304 (2020).
- [36] B. Bertini, P. Kos, and T. c. v. Prosen, Exact correlation functions for dual-unitary lattice models in 1 + 1 dimensions, *Phys. Rev. Lett.* **123**, 210601 (2019).
- [37] M. P. Fisher, V. Khemani, A. Nahum, and S. Vijay, Random quantum circuits, *Annual Review of Condensed Matter Physics* **14**, 335 (2023).
- [38] A. Nahum, S. Vijay, and J. Haah, Operator spreading in random unitary circuits, *Phys. Rev. X* **8**, 021014 (2018).
- [39] A. W. Harrow and R. A. Low, Random quantum circuits are approximate 2-designs, *Communications in Mathematical Physics* **291**, 257 (2009).
- [40] L. Levi, Y. Krivolapov, S. Fishman, and M. Segev, Hyper-transport of light and stochastic acceleration by evolving disorder, *Nature Physics* **8**, 912 (2012).
- [41] J. C. Hoke, M. Ippoliti, D. Abanin, R. Acharya, M. Ansmann, F. Arute, K. Arya, A. Asfaw, J. Atalaya, J. C. Bardin, *et al.*, Quantum information phases in space-time: measurement-induced entanglement and teleportation on a noisy quantum processor, *arXiv preprint arXiv:2303.04792* (2023).
- [42] X. Mi, M. Ippoliti, C. Quintana, A. Greene, Z. Chen, J. Gross, F. Arute, K. Arya, J. Atalaya, R. Babbush, *et al.*, Time-crystalline eigenstate order on a quantum processor, *Nature* **601**, 531 (2022).
- [43] J. De Nardis, S. Gopalakrishnan, R. Vasseur, and B. Ware, Stability of superdiffusion in nearly integrable spin chains, *Phys. Rev. Lett.* **127**, 057201 (2021).
- [44] P. W. Claeys, A. Lamacraft, and J. Herzog-Arbeitman, Absence of superdiffusion in certain random spin models, *Phys. Rev. Lett.* **128**, 246603 (2022).
- [45] P. Glorioso, L. Delacrétaz, X. Chen, R. Nandkishore, and A. Lucas, Hydrodynamics in lattice models with continuous non-abelian symmetries, *SciPost Physics* **10**, 015 (2021).
- [46] We drop the subscript  $k$  because we solve the operator equations for fixed momentum.
- [47] T. Can, V. Oganesyan, D. Orgad, and S. Gopalakrishnan, Spectral gaps and midgap states in random quantum master equations, *Phys. Rev. Lett.* **123**, 234103 (2019).
- [48] W. Chen, M. Abbasi, B. Ha, S. Erdamar, Y. N. Joglekar, and K. W. Murch, Decoherence-induced exceptional points in a dissipative superconducting qubit, *Phys. Rev. Lett.* **128**, 110402 (2022).
- [49] D. S. Bhakuni, S. Dattagupta, and A. Sharma, Effect of noise on bloch oscillations and wannier-stark localization, *Phys. Rev. B* **99**, 155149 (2019).
- [50] M. Bandyopadhyay, S. Dattagupta, and A. Dubey, Effect of noise on quantum transport of a charged particle in a tight-binding lattice, *Phys. Rev. B* **101**, 184308 (2020).
- [51] G. H. Wannier, Dynamics of band electrons in electric and magnetic fields, *Rev. Mod. Phys.* **34**, 645 (1962).
- [52] D. Emin and C. F. Hart, Existence of wannier-stark localization, *Phys. Rev. B* **36**, 7353 (1987).
- [53] E. E. Mendez, F. Agulló-Rueda, and J. M. Hong, Stark localization in gaas-gaalas superlattices under an electric field, *Phys. Rev. Lett.* **60**, 2426 (1988).
- [54] C. Schmidt, J. Bühler, A.-C. Heinrich, J. Allerbeck, R. Podzinski, D. Berghoff, T. Meier, W. G. Schmidt, C. Reichl, W. Wegscheider, *et al.*, Signatures of transient wannier-stark localization in bulk gallium arsenide, *Nature Communications* **9**, 2890 (2018).
- [55] A. Amir, Y. Lahini, and H. B. Perets, Classical diffusion of a quantum particle in a noisy environment, *Phys. Rev. E* **79**, 050105 (2009).
- [56] D. Evensky, R. Scalettar, and P. G. Wolynes, Localization and dephasing effects in a time-dependent anderson hamiltonian, *Journal of Physical Chemistry* **94**, 1149 (1990).
- [57] S. Lorenzo, T. Apollaro, G. M. Palma, R. Nandkishore, A. Silva, and J. Marino, Remnants of anderson localization in prethermalization induced by white noise, *Phys. Rev. B* **98**, 054302 (2018).
- [58] T. LM Lezama and Y. Bar Lev, Logarithmic, noise-induced dynamics in the anderson insulator, *SciPost Physics* **12**, 174 (2022).
- [59] S. Marcantoni, F. Carollo, F. M. Gambetta, I. Lesanovsky, U. Schneider, and J. P. Garrahan, Anderson and many-body localization in the presence of spatially correlated classical noise, *Phys. Rev. B* **106**, 134211 (2022).

# Supplemental Material for Noise Induced Universal Diffusive Transport in Fermionic Chains

Christopher M. Langlett<sup>1</sup> and Shenglong Xu<sup>1</sup>

<sup>1</sup>*Department of Physics & Astronomy, Texas A&M University, College Station, Texas 77843, USA*

In this Supplementary Material, we provide detailed derivations of the equations given in the main text. We begin by solving the noise-free case using standard free fermion techniques. This section is followed by deriving the operator equation upon which we demonstrate the noise averaging. The remaining sections illustrate how to derive the differential equations for the coefficients when the effective Lindblad is nearest-neighbor with static hopping, where we then explicitly solve for the bound state energy in detail. We repeat this procedure when the effective Lindblad is onsite, i.e., the noise couples to the density.

## CONTENTS

S1. Fermion Operator Identities.	1
S2. Free-Fermion Methods.	2
A. Efficient Free-Fermion Simulation.	3
S3. Operator Equation of Motion.	4
S4. Time Dependent Hopping.	5
A. Coherent Term	5
B. Incoherent Term.	6
C. Operator Equation of Motion.	7
D. Mapping to $\ell$ and $\mathcal{R}$ .	7
E. Finite Noise Solution.	8
F. Finite Noise Solution with Linear Potential.	9
1. Approximate solution to Bound State Energy.	10
G. Numerical Methods for Determining the Coefficients.	11
S5. Time-Dependent Potential.	12
A. Incoherent Term	12
B. Mapping to $\ell$ and $\mathcal{R}$	13
C. Solving Ground State Eigenvalue Problem	14

## S1. FERMION OPERATOR IDENTITIES.

In this appendix, we provide helpful fermion operator identities used to derive the equations of motion. We denote the spinless fermionic creation and annihilation operators by  $(c_\alpha^\dagger, c_\alpha)$ , where  $\alpha$  indicates the site index. These operators obey the algebra,

$$\begin{aligned} \{c_\alpha, c_\beta\} &= \{c_\alpha^\dagger, c_\beta^\dagger\} = 0 \\ \{c_\alpha^\dagger, c_\beta\} &= \delta_{\alpha,\beta}. \end{aligned} \tag{S1}$$

Further, defining the density operator  $n_\alpha = c_\alpha^\dagger c_\alpha$ , we obtain,

$$\begin{aligned} [n_\alpha, c_\beta] &= -\delta_{\alpha,\beta} c_\beta, & [n_\alpha, c_\beta^\dagger] &= \delta_{\alpha,\beta} c_\beta^\dagger \\ \{n_\alpha, c_\beta^\dagger\} &= \delta_{\alpha,\beta} c_\alpha^\dagger + 2c_\beta^\dagger n_\alpha, & \{n_\alpha, c_\beta\} &= \delta_{\alpha,\beta} c_\alpha + 2n_\alpha c_\beta \end{aligned} \tag{S2}$$

These relations were utilized in deriving the differential equations for the coefficients in the operator expansion.

## S2. FREE-FERMION METHODS.

In this appendix, we give an overview of calculating the density-density correlation function using standard methods that compare the operator expansion technique used in the main text. In the no noise limit,  $\Gamma_{xy} = 0$ , with  $J_{x,x} = 0$ , the exchange couplings are uniform, and the Hamiltonian describes a one-dimensional free-fermion. At this point, the Hamiltonian regains spatial and time translation invariance, thereby in Fourier space, the fermionic operators become,

$$\begin{aligned} c_x &= \frac{1}{\sqrt{N}} \sum_k e^{ik \cdot x} c_k \\ c_x^\dagger &= \frac{1}{\sqrt{N}} \sum_k e^{-ik \cdot x} c_k^\dagger \end{aligned} \quad (\text{S3})$$

here  $k$  is the momentum of the first Brillouin zone, and the Hamiltonian,

$$H = \sum_k \mathcal{E}_k c_k^\dagger c_k \quad (\text{S4})$$

with the band dispersion,  $\mathcal{E}_k = 2 \cos(k)$  (lattice spacing  $a = 1$ ). In the momentum basis, time-evolution of the operators  $c_k^\dagger(c_k)$  is simple, taking the form,

$$\begin{aligned} c_k(t) &= e^{-i\mathcal{E}_k t} c_k \\ c_k^\dagger(t) &= e^{i\mathcal{E}_k t} c_k^\dagger. \end{aligned} \quad (\text{S5})$$

In real space, we have that  $c_x(t) = \sum_y u(x-y, t) c_y$ . The function,  $u(x-y, t)$ , is the Fourier transform of  $e^{-i\mathcal{E}_k t}$ , and controls how the correlation function grows in time. Specifically, for the model at hand, the envelope function takes the form,

$$c_x(t) = \sum_y \underbrace{\left[ \frac{1}{N} \sum_k e^{i(x-y)k} e^{-i\mathcal{E}_k t} \right]}_{u(x-y, t)} c_y. \quad (\text{S6})$$

We now study the universal properties of this function. In the thermodynamic limit, the mode functions take the form,

$$\begin{aligned} u(x-y, t) &= \int_{-\pi}^{\pi} \frac{dk}{2\pi} e^{i(x-y)k} e^{-2i \cos(k)t} \\ &= i^{(x-y)} \mathcal{J}_{x-y}(2t). \end{aligned} \quad (\text{S7})$$

In the previous equation,  $\mathcal{J}_\alpha(2t)$  is a Bessel function of the first kind of order  $\alpha$ . Utilizing the above result in combination with Eq. (S6), the time-evolved operators become

$$c_x(t) = \sum_y i^{(x-y)} \mathcal{J}_{x-y}(2t) c_y. \quad (\text{S8})$$

Transport is determined by determining the late-time behavior of the density-density correlation function. First, write the time-evolved density operator,

$$n_x(t) = \sum_{\alpha, \beta} (i)^{\alpha-\beta} \mathcal{J}_{x-\alpha}(2t) \mathcal{J}_{x-\beta}(2t) c_\alpha^\dagger c_\beta. \quad (\text{S9})$$

Recall from the main text that the correlation function is defined as,

$$C_{xy}(t) = \frac{1}{2^N} \text{tr}(n_x(t) n_y(0)) - \frac{1}{4}. \quad (\text{S10})$$

By inserting Eq. (S9) into the previous equation, we find,

$$\begin{aligned} C_{x,y}(t) &= \frac{1}{2^N} \sum_{\alpha, \beta, \gamma, \delta} [i^{\alpha-\beta+\gamma-\delta} \mathcal{J}_{x-\alpha}(2t) \mathcal{J}_{x-\beta}(2t) \mathcal{J}_{y-\gamma}(0) \mathcal{J}_{y-\delta}(0)] \text{tr}(c_\alpha^\dagger c_\beta c_\gamma^\dagger c_\delta) - \frac{1}{4} \\ &= \frac{1}{2^N} \sum_{\alpha, \beta} [i^{\alpha-\beta} \mathcal{J}_{x-\alpha}(2t) \mathcal{J}_{x-\beta}(2t)] \text{tr}(c_\alpha^\dagger c_\beta n_y) - \frac{1}{4}. \end{aligned} \quad (\text{S11})$$



we utilized the relation  $\mathcal{J}_{\alpha-\beta}(0) = \delta_{\alpha,\beta}$  when moving between lines. In the previous equation,  $C_{x,y} = 0$  when  $\alpha \neq \beta$ , in which the sum breaks into two separate cases: (i)  $\alpha \neq y$  and (ii)  $\alpha = y$ . Finally, using the identity  $\sum_{\alpha=-\infty}^{\infty} \mathcal{J}_{x-\alpha}^2(z) = 1$ , we evaluate the correlation function to be,

$$C_{x,y}(t) = \frac{1}{4} \mathcal{J}_{x-y}^2(2t). \quad (\text{S12})$$

To compare our analytical result to simulations, we utilize the non-interacting structure of the model to simulate large systems to late time, enabling reliable extraction hydrodynamic behavior. The following section focuses on efficiently implementing free-fermion numerics to compute the correlation function.

### A. Efficient Free-Fermion Simulation.

The Hamiltonian in the many-body basis is stored as a  $2^N \times 2^N$  matrix, severely limiting the possible system size. However, by utilizing the non-interacting structure, we can simulate the dynamics in the single particle basis; the Hamiltonian is a  $N \times N$  matrix. This allows us to simulate large systems, but we are hampered numerically by the time scale as we need to diagonalize the Hamiltonian at each time step. For the system to remain uncorrelated in time, it is crucial for  $dt$  to be small. We now outline how to compute  $C_{xy}(t)$  numerically in the single particle basis in an efficient manner. We begin with the general Hamiltonian,

$$H = \sum_{ij} c_i^\dagger M_{ij} c_j. \quad (\text{S13})$$

Here, the matrix  $M$  is a  $N \times N$  real symmetric matrix that is diagonalized as  $M = V D V^T$  where  $V$  are the eigenvectors satisfying  $V V^T = \mathbb{1}$  and  $D = \text{diag}(\lambda_1, \dots, \lambda_N)$  is a diagonal matrix. The Hamiltonian now becomes,

$$H = \sum_{ij} \sum_{kl} c_i^\dagger V_{ik} \lambda_k V_{jl} c_j \quad (\text{S14})$$

$$= \sum_k \lambda_k d_k^\dagger d_k. \quad (\text{S15})$$

The normal mode operators,  $d_k = \sum_j V_{jk} c_j$  and  $d_k^\dagger = \sum_i c_i^\dagger V_{ik}$  inherit the standard fermionic anti-commutation relations. We now define the vectors,  $\hat{d}^\dagger = (d_1^\dagger, \dots, d_N^\dagger) = \hat{c}^\dagger V$  and  $\hat{d} = (d_1, \dots, d_N)^T = V^T \hat{c}$ . From the Heisenberg evolution of the normal mode operators, we determine the original fermion operators evolve as,

$$\hat{c}^\dagger(t) = \hat{c}^\dagger (V e^{iDt} V^T) \quad (\text{S16})$$

$$\hat{c}(t) = (V e^{iDt} V^T) \hat{c} \quad (\text{S17})$$

The correlation function becomes,

$$C_{xx}(t) = \frac{1}{2^N} \text{tr}(n_x(t) n_x) - \frac{1}{4} \quad (\text{S18})$$

$$= \frac{1}{2^N} \left( \sum_{\sigma,\rho} \sum_{\mu,\nu} (V_{\sigma\rho} e^{i\lambda_\rho t} V_{\rho x}^T) (V_{x\mu} e^{-i\lambda_\mu t} V_{\mu\nu}^T) \text{tr}(c_\sigma^\dagger c_\nu c_x^\dagger c_x) \right) - \frac{1}{4} \quad (\text{S19})$$

$$= \frac{1}{2^N} \left( \frac{2^N}{2} \sum_{\rho,\mu} V_{x\rho} V_{\rho x}^T V_{x\mu} V_{\mu x}^T e^{i\omega_{\rho\mu} t} + \frac{2^N}{4} \sum_{\rho,\sigma,\mu} V_{\sigma\rho} V_{\rho x}^T V_{x\mu} V_{\mu\sigma}^T e^{i\omega_{\rho\mu} t} \right) - \frac{1}{4} \quad (\text{S20})$$

$$= \frac{1}{2} a_{x,x}(t) a_{x,x}^*(t) + \frac{1}{4} \sum_{\sigma,\sigma \neq x} a_{\sigma,x}(t) a_{x,\sigma}^*(t) - \frac{1}{4}. \quad (\text{S21})$$

Where above we have defined the time-dependent amplitudes,  $a_{m,n}(t) = \sum_k V_{m,k} e^{i\lambda_k t} V_{k,n}^T$ . Moving from the first to the second line, we utilized that  $\text{tr}(c_\sigma^\dagger c_\nu c_x^\dagger c_x) = 0$  if  $\sigma \neq \nu$ . The correlation function decomposes into two cases in the third line:  $\sigma = x$  and  $\sigma \neq x$  where we used the relations  $\text{tr}(n_\sigma) = 2^N/2$  and  $\text{tr}(n_\sigma n_x) = 2^N/4$  and defined the energy difference,  $\omega_{\rho\mu} = \lambda_\rho - \lambda_\mu$ . Efficient time evolution is performed as follows:

Step 1: At each  $dt$  draw  $N - 1$  random numbers from the Gaussian distribution with a mean  $\mu = \sin(\theta)$  and standard deviation  $\sigma = (\cos(\theta)/dt)^{1/2}$ .

Step 2: Diagonalize the  $N \times N$  Hamiltonian.

Step 3: Compute the correlation function  $C_{xx}(dt)$  from the eigenvalues and eigenvectors.

Step 4: Repeat the above steps for *each* time-step.

Step 5: Repeat the entire procedure a designated number of disorder realizations and average.

As an aside, for simulating the Brownian potential in the first step replace  $N - 1$  with  $N$  random numbers.

### S3. OPERATOR EQUATION OF MOTION.

This first appendix outlines the derivation for the operator equation of motion due to a stochastically varying Hamiltonian. Consider a chain of  $N$  non-interacting fermions governed by the Hamiltonian in the main text. We consider the Brownian couplings,  $\Gamma_{x,y}(t)$ , which are time-dependent real Gaussian numbers with a mean and variance are given by,

$$\begin{aligned}\mathbb{E}[\Gamma_{i,j}(t)] &= 0 \\ \mathbb{E}[\Gamma_{i,j}(t)\Gamma_{l,m}(t')] &= \Gamma_{x,y}\delta_{i,t}\delta_{j,m}\delta(t-t').\end{aligned}\tag{S22}$$

Where the operation  $\mathbb{E}[\cdot]$  denotes the Gaussian average couplings,  $\Gamma_{x,y}$  sets the energy scale, and  $\delta(t-t')$  implies that the couplings are correlated at a single instance in time.

We expand the flow of the Heisenberg operator up to order  $dt^2$  because the variance is of order  $dt^{-1}$ . Specifically, consider the Heisenberg evolution of an operator  $\mathcal{O}$ ,

$$\begin{aligned}\mathcal{O}(t+dt) &= \mathcal{U}_{dt}\mathcal{O}(t)\mathcal{U}_{dt}^\dagger \\ &= \mathcal{O}(t) + i[H_t, \mathcal{O}]dt + \mathcal{L}[\mathcal{O}]dt^2\end{aligned}\tag{S23}$$

With the unitary operator,  $\mathcal{U}_{dt} = e^{-iH_t dt}$  and the effective Lindblad,  $\mathcal{L}[\mathcal{O}] = H_t^\dagger \mathcal{O} H_t - \frac{1}{2}\{H_t^\dagger H_t, \mathcal{O}\}$ . Inserting the Hamiltonian into the operator equation, we get,

$$\mathcal{O}(t+dt) = \mathcal{O}(t) + \sum_{x,y} i \left[ J_{x,y} [c_x^\dagger c_y, \mathcal{O}] + \Gamma_{x,y}(t) [c_x^\dagger c_y, \mathcal{O}] \right] dt + \mathcal{L}_{x,y}[\mathcal{O}] dt^2\tag{S24}$$

The Lindblad term breaks into terms with the coefficients  $J_{x,y} J_{x,y}$ ,  $J_{x,y} \Gamma_{x,y}(t)$ ,  $\Gamma_{x,y}(t) \Gamma_{x,y}(t)$ , moreover, only the first and final term survive noise averaging. We now average over disorder realizations,

$$d\bar{\mathcal{O}}_t = \sum_{x,y} i \left[ J_{x,y} [c_x^\dagger c_y, \bar{\mathcal{O}}_t] + \mathbb{E}[\Gamma_{x,y}(t)] [c_x^\dagger c_y, d\bar{\mathcal{O}}_t] \right] dt + \left[ \mathbb{E}[\Gamma_{x,y}(t) \Gamma_{x,y}(t)] \mathcal{L}_{x,y}[\bar{\mathcal{O}}_t] + J_{x,y} J_{x,y} \mathcal{L}_{x,y}[\bar{\mathcal{O}}_t] \right] dt^2\tag{S25}$$

$$= \sum_{x,y} i J_{x,y} [c_x^\dagger c_y, \bar{\mathcal{O}}_t] dt + \Gamma_{x,y} \mathcal{L}_{x,y}[\bar{\mathcal{O}}_t] dt + J_{x,y} J_{x,y} \mathcal{L}_{x,y}[\bar{\mathcal{O}}_t] dt^2.\tag{S26}$$

Only keeping terms that are of order  $dt$ , leads to the noise-averaged operator equation,

$$\frac{d\bar{\mathcal{O}}_t}{dt} = \sum_{x,y} \left[ i J_{x,y} [c_x^\dagger c_y, \bar{\mathcal{O}}_t] + \Gamma_{x,y} \mathcal{L}_{x,y}[\bar{\mathcal{O}}_t] \right]\tag{S27}$$

Where we have defined  $\mathbb{E}(d\mathcal{O}) = d\bar{\mathcal{O}}$  and the Lindblad has the form,  $\mathcal{L}_{x,y}[\bar{\mathcal{O}}] = L_{x,y}^\dagger \bar{\mathcal{O}} L_{x,y} - \frac{1}{2}\{L_{x,y}^\dagger L_{x,y}, \bar{\mathcal{O}}\}$ . Generically, the above equation applies for long-range hopping, however, we consider either onsite or nearest-neighbor interactions. Specifically, when the noise is coupled to nearest-neighbor hopping ( $y = x + 1$ ) then the jump operator is  $L_{x,x+1} = c_x^\dagger c_{x+1} + c_{x+1}^\dagger c_x$ , whereas, when the noise is coupled to the density  $L_{x,x} = n_x$  where  $n_x$  is the fermion

density operator. We now list all the different variations of Eq. (S27) solved in the main-text,

$$\begin{aligned}
d\bar{\mathcal{O}}_t &= iJ \sum_x [L_{x,x+1}, \bar{\mathcal{O}}_t] dt : \text{Noise-free: } J_{x,x+1} = J, \Gamma_{x,y} = 0 \\
d\bar{\mathcal{O}}_t &= \sum_x \Gamma_{x,x+1} \mathcal{L}_{x,x+1}[\bar{\mathcal{O}}_t] dt : \text{Strong Noise Hopping: } J_{x,y} = \Gamma_{x,x} = 0 \\
d\bar{\mathcal{O}}_t &= \sum_x \left[ iV_x [n_x, \bar{\mathcal{O}}_t] + \Gamma_{x,x+1} \mathcal{L}_{x,x+1}[\bar{\mathcal{O}}_t] \right] dt : J_{x,x+1} = \Gamma_{x,x} = 0, J_{x,x} = V_x \\
d\bar{\mathcal{O}}_t &= \sum_x \left[ iJ [L_{x,x+1}, \bar{\mathcal{O}}_t] + \Gamma_{x,x} \mathcal{L}_{x,x}[\bar{\mathcal{O}}_t] \right] dt : J_{x,x+1} = J, J_{x,x} = \Gamma_{x,x+1} = 0 \\
d\bar{\mathcal{O}}_t &= \sum_x \left[ i \sin(\theta) [L_{x,x+1}, \bar{\mathcal{O}}_t] + \cos(\theta) \mathcal{L}_{x,x+1}[\bar{\mathcal{O}}_t] \right] dt : J_{x,x+1} = \sin(\theta), J_{x,x} = 0 = \Gamma_{x,x}, \Gamma_{x,x+1} = \cos(\theta) \\
d\bar{\mathcal{O}}_t &= \sum_x \left[ i \sin(\theta) [L_{x,x+1}, \bar{\mathcal{O}}_t] - i\gamma x [n_x, \bar{\mathcal{O}}_t] + \cos(\theta) \mathcal{L}_{x,x+1}[\bar{\mathcal{O}}_t] \right] dt : J_{x,x} = V_x = -\gamma x.
\end{aligned} \tag{S28a}$$

The first equation is the noise-free limit where the operator dynamics are that of a free fermion which we solve in the first section. The second equation is the opposite limit, where the dynamics are purely incoherent due to noise only. It is important to note that the operator equation of the first equation is anti-hermitian, while the second is hermitian. When the equation has a static and noisy term, the equation is generically non-hermitian. Moreover, the final four equations map onto the dynamics of an effective one-dimensional non-hermitian hopping model.

#### S4. TIME DEPENDENT HOPPING.

In this section, we derive the differential equation for the operator coefficients where the drive is on nearest-neighbor hopping, i.e.,  $\Gamma_{x,y} = \Gamma_{x,x+1} = \Gamma$ , which competes with an arbitrarily strong static hopping,  $J_{x,x} = 0, J_{x,x+1} = J$ . We begin by deriving the contribution from the coherent evolution followed by then the incoherent term. We then solve various aspects of the full equation, including the finite noise bound state, real part of the spectrum, and the case of a linear potential.

##### A. Coherent Term

We begin with the time averaged operator equation of motion,

$$\frac{d\bar{n}_t}{dt} = \sum_x \left[ iJ [L_{x,x+1}, \bar{n}_t] + \Gamma \mathcal{L}_{x,x+1}[\bar{n}_t] \right]. \tag{S29}$$

In this section, we derive the term from the unitary dynamics,

$$\begin{aligned}
[c_x^\dagger c_{x+1}, \bar{n}_t] &= \sum_x \sum_{mn} A_{m,n} \left[ c_x^\dagger [c_{x+1}, c_m^\dagger] c_n + [c_x^\dagger, c_m^\dagger] c_{x+1} c_n + c_m^\dagger c_x^\dagger [c_{x+1}, c_n] + c_m^\dagger [c_x^\dagger, c_n] c_{x+1} \right] \\
&= \sum_x \sum_{mn} A_{m,n} \left[ c_x^\dagger (2c_{x+1} c_m^\dagger - \delta_{x+1,m}) c_n + 2c_x^\dagger c_m^\dagger c_{x+1} c_n \right. \\
&\quad \left. + 2c_m^\dagger c_x^\dagger c_{x+1} c_n + c_m^\dagger (2c_x c_n^\dagger - \delta_{x,n}) c_{x+1} \right] \\
&= \sum_x \sum_{m,n} A_{m,n} \left[ 2c_x^\dagger c_{x+1} c_m^\dagger c_n - \delta_{x+1,m} c_x^\dagger c_n + 2c_m^\dagger c_x^\dagger c_n c_{x+1} - \delta_{x,n} c_m^\dagger c_{x+1} \right] \\
&= \sum_x \sum_{m,n} A_{m,n} \left[ \delta_{x+1,m} c_x^\dagger c_n - \delta_{x,n} c_m^\dagger c_{x+1} \right].
\end{aligned} \tag{S31}$$

In the first line, we utilized a commutator identity between four operators and then used that  $[A, B] = 2AB - \{A, B\}$  where we then applied the anti-commutator relation for fermion operators. For the second line, the product of four

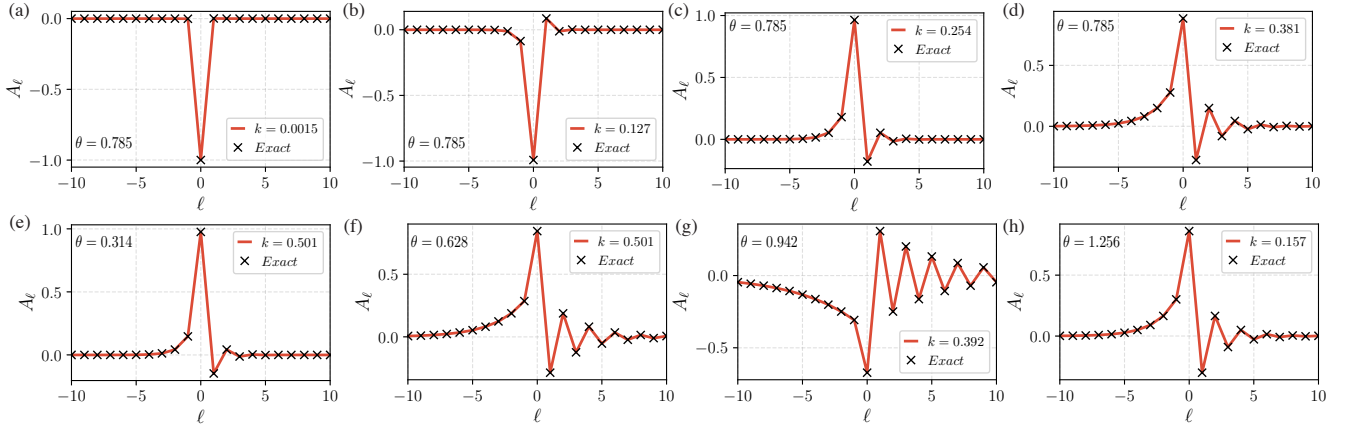


FIG. S1. *Hydrodynamic Mode Ansatz*. (a)-(d) Plot of the bound state coefficient  $A_{\ell,k}$  for the case of finite noise time dependent hopping. Each figure is evaluated at a different center-of-mass momentum  $k$ . The black crosses are from diagonalization of the eigenvalue equations, while the red curves are the analytical result. (e)-(h) Same as the first row except we vary the noise strength and chose  $k$  to be the value right before the bound-to-scattering state phase transition. Parameters:  $N = 8000$ ,  $\ell_{\max} = N/2$ .

fermion operators cancels by anti-commuting the creation operators and then expand in the third line. Because the model is non-interacting the final result cannot have more than a product of two fermion operators, thus we simplify further using the anti-commutation relation  $\{c_m^\dagger, c_{x+1}\}$  and end with the final equation. The second commutator is found by a similar calculation or by setting  $x+1 \rightarrow x$  and  $x \rightarrow x+1$  in the above equation,

$$[c_{x+1}^\dagger c_x, \bar{n}_t] = \sum_x \sum_{mn} A_{m,n} \left[ \delta_{x,m} c_{x+1}^\dagger c_n - \delta_{x+1,n} c_m^\dagger c_x \right]. \quad (\text{S32})$$

Moreover, we find the final equation after resolving the delta functions is,

$$iJ \sum_x [L_{x,x+1}, \bar{n}_t] = iJ \sum_{m,n} A_{m,n} \left[ c_{m-1}^\dagger c_n - c_m^\dagger c_{n+1} + c_{m+1}^\dagger c_n - c_m^\dagger c_{n-1} \right] \quad (\text{S33})$$

Next, we want to shift the indices so that each operator is equivalently  $c_m^\dagger c_n$  which allow us to equate sides and get a differential equation for  $A_{m,n}$ .

$$\begin{aligned} A_{m,n} c_{m-1}^\dagger c_n &\rightarrow A_{m+1,n} c_m^\dagger c_n, & A_{m,n} c_m^\dagger c_{n+1} &\rightarrow A_{m,n-1} c_m^\dagger c_n \\ A_{m,n} c_{m+1}^\dagger c_n &\rightarrow A_{m-1,n} c_m^\dagger c_n, & A_{m,n} c_m^\dagger c_{n-1} &\rightarrow A_{m,n+1} c_m^\dagger c_n \end{aligned} \quad (\text{S34})$$

The final equation due to unitary dynamics is,

$$iJ \sum_x [L_{x,x+1}, \bar{n}_t] = iJ \sum_{mn} \left[ A_{m+1,n} - A_{m,n-1} + A_{m-1,n} - A_{m,n+1} \right] c_m^\dagger c_n \quad (\text{S35})$$

In the next section, we derive the contribution from the effective Lindblad term.

## B. Incoherent Term.

In this section, we derive the incoherent piece that arises from the variance of the couplings,

$$\sum_x \mathcal{L}_{x,x}[\bar{n}_t] = \sum_x \sum_{m,n} A_{m,n} \left[ L_{x,x+1}^\dagger c_m^\dagger c_n L_{x,x+1} - \frac{1}{2} \{L_{x,x+1}^\dagger L_{x,x+1}, c_m^\dagger c_n\} \right]. \quad (\text{S36})$$

where  $L_{x,x+1} = c_x^\dagger c_{x+1} + c_{x+1}^\dagger c_x$ . After some algebra and using fermion identities, we get the final equation,

$$\frac{d\bar{n}_t}{dt} = \sum_{mn} \left[ -2A_{m,n} c_m^\dagger c_n + A_{m,n} \delta_{m,n-1} c_m^\dagger c_{n-1} + A_{m,n} \delta_{m,n+1} c_m^\dagger c_{n+1} + A_{m,n} \delta_{m,n} (n_{m+1} + n_{m-1}) \right] \quad (\text{S37})$$

Next, we want to shift the indices so that each operator is aligned with  $c_m^\dagger c_n$  which allow us to equate sides and get a differential equation for  $A_{m,n}$ .

$$\begin{aligned} A_{m,n} \delta_{m,n} c_{m-1}^\dagger c_{m-1} &\rightarrow A_{m+1,n+1} \delta_{m,n} c_m^\dagger c_n, & A_{m,n} \delta_{m,n} c_{m+1}^\dagger c_{m+1} &\rightarrow A_{m-1,n-1} \delta_{m,n} c_m^\dagger c_n \\ A_{m,n} \delta_{m,n+1} c_n^\dagger c_{n+1} &\rightarrow A_{m+1,n-1} \delta_{m+1,n} c_m^\dagger c_n, & A_{m,n} \delta_{m,n-1} c_n^\dagger c_{n-1} &\rightarrow A_{m-1,n+1} \delta_{m-1,n} c_m^\dagger c_n \end{aligned} \quad (\text{S38})$$

The operator equation of motion becomes,

$$\frac{d\bar{n}_t}{dt} = \sum_{m,n} \left[ -2A_{m,n} + \delta_{m+1,n} A_{m+1,n-1} + \delta_{m-1,n} A_{m-1,n+1} + \delta_{m,n} A_{m+1,n+1} + \delta_{m,n} A_{m-1,n-1} \right] c_m^\dagger c_n. \quad (\text{S39})$$

Moreover, we find that the contribution from the incoherent piece is as follows,

$$\frac{dA_{m,n}}{dt} = \left[ -2A_{m,n} + \delta_{m+1,n} A_{m+1,n-1} + \delta_{m-1,n} A_{m-1,n+1} + \delta_{m,n} A_{m+1,n+1} + \delta_{m,n} A_{m-1,n-1} \right] \quad (\text{S40})$$

In the following section we will perform the mapping to the operator length and center-of-mass coordinates.

### C. Operator Equation of Motion.

Combining, the equation from the previous two sections, we arrive at the full operator equation,

$$\begin{aligned} \partial_t A_{m,n} &= iJ \left[ A_{m+1,n} - A_{m,n+1} + A_{m-1,n} - A_{m,n-1} \right] \\ &+ \Gamma \left[ -2A_{m,n} + \delta_{m+1,n} A_{m+1,n-1} + \delta_{m-1,n} A_{m-1,n+1} + \delta_{m,n} A_{m-1,n-1} + \delta_{m,n} A_{m+1,n+1} \right]. \end{aligned} \quad (\text{S41})$$

When a static potential is included in the coherent dynamics, the additional term is  $i[V_m - V_n]A_{m,n}$  which has no affect in the strong noise limit.

### D. Mapping to $\ell$ and $\mathcal{R}$ .

Spatial translation invariance is partially restored in a different coordinate system defined by the variables  $\ell = n - m$  and  $\mathcal{R} = n + m$ . Here  $\ell$  represents the length of the operator and  $\mathcal{R}$  the center-of-mass of the operator. The coefficients under this mapping become,

$$\begin{aligned} A_{m+1,n-1} &\xrightarrow{(n-1-m-1=\ell-2, n-1+m+1=\mathcal{R})} A_{\ell-2,\mathcal{R}}, & A_{m-1,n+1} &\xrightarrow{(n+1-m+1=\ell+2, n+1+m-1=\mathcal{R})} A_{\ell+2,\mathcal{R}} \\ A_{m+1,n+1} &\xrightarrow{(n+1-m-1=\ell, n+1+m+1=\mathcal{R}+2)} A_{\ell,\mathcal{R}+2}, & A_{m-1,n-1} &\xrightarrow{(n-1-m+1=\ell, n-1+m-1=\mathcal{R}-2)} A_{\ell,\mathcal{R}-2} \\ \delta_{m+1,n} &\xrightarrow{(\ell=1)} \delta_{\ell,1}, & \delta_{m-1,n} &\xrightarrow{\ell=-1} \delta_{\ell,-1} \end{aligned} \quad (\text{S42})$$

$$(\text{S43})$$

Applying this transformation to the equation above,

$$\begin{aligned} \partial_t A_{\ell,\mathcal{R}} &= iJ \left[ A_{\ell-1,\mathcal{R}+1} - A_{\ell+1,\mathcal{R}+1} + A_{\ell+1,\mathcal{R}-1} - A_{\ell-1,\mathcal{R}-1} \right] \\ &+ \Gamma \left[ -2A_{\ell,\mathcal{R}} + \delta_{\ell,1} A_{\ell-2,\mathcal{R}} + \delta_{\ell,-1} A_{\ell+2,\mathcal{R}} + \delta_{\ell,0} (A_{\ell,\mathcal{R}+2} + A_{\ell,\mathcal{R}-2}) \right] \end{aligned} \quad (\text{S44})$$

Now the above equation is simplified further by looking at the terms  $\delta_{\ell,-1} A_{\ell+2,\mathcal{R}}$  and  $\delta_{\ell,1} A_{\ell-2,\mathcal{R}}$  which are nonzero if  $\ell = \pm 1$  with the coefficients  $A_{\mp 1}$ . A similar argument can be made for  $\delta_{\ell,0} (A_{\ell,\mathcal{R}+2} + A_{\ell,\mathcal{R}-2})$ . Moreover, the final equation is,

$$\begin{aligned} \partial_t A_{\ell,\mathcal{R}} &= iJ \left[ A_{\ell-1,\mathcal{R}+1} - A_{\ell+1,\mathcal{R}+1} + A_{\ell+1,\mathcal{R}-1} - A_{\ell-1,\mathcal{R}-1} \right] \\ &+ \Gamma \left[ -2A_{\ell,\mathcal{R}} + \delta_{\ell,1} A_{-1,\mathcal{R}} + \delta_{\ell,-1} A_{1,\mathcal{R}} + \delta_{\ell,0} (A_{0,\mathcal{R}+2} + A_{0,\mathcal{R}-2}) \right] \end{aligned} \quad (\text{S45})$$

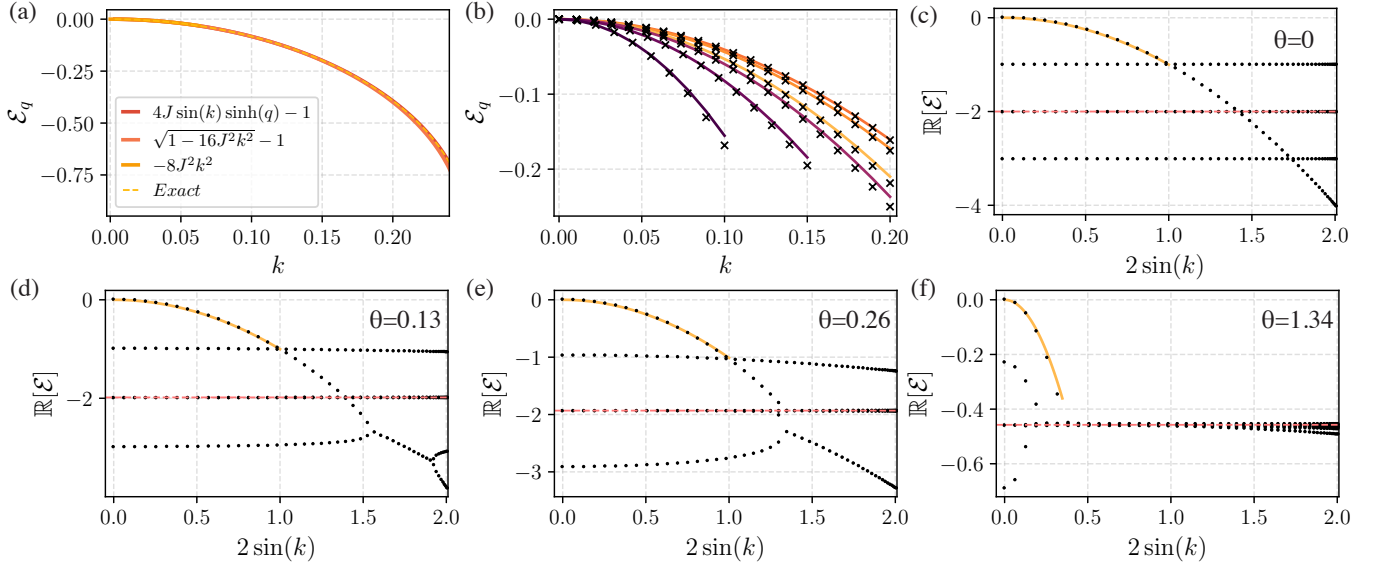


FIG. S2. *Bound State Energy*. (a) The bound state energy for the noisy potential with static hopping. The dotted orange line is from diagonalizing the eigenvalue equation with the other curves representing different stages in approximating the low momentum scaling. (b) Bound state energy for noisy hopping with different strengths, the black crosses are from diagonalization of the eigenvalue equation Eq. (S47) and the solid curves are the analytical result. (c)-(f) We illustrate the real part of the eigenvalue spectrum for finite noise. At small momentum, the largest real eigenvalue is the diffusive bound state Eq. (S56), which at larger momentum crosses over to a scattering state given by the red line. Increasing  $k$  further reveals that the bound state reemerges at an exceptional point. Before the exceptional point, the cubic equation admits two physical solutions with real energies, which then coalesce and become a conjugate pair of complex energies. Interestingly, near the strong drive limit is a reentrant-like point [see (d)] where degeneracy is re-broken, and the purely real energies emerge once more. Parameters: (a)  $N = 4000$ ,  $\Gamma/J = 1$ , (b)  $N = 4000$ ,  $\theta = [0, \dots, 1.34]$ , and (c)-(f)  $N = 4000$ ,  $\ell_{\max} = N/2$ , and the red line is at  $2 \cos(\theta)$ .

Now because the delta functions are independent of  $\mathcal{R}$  we can perform a discrete Fourier transformation in this coordinate, namely,  $A_{\ell, \mathcal{R}} = \sum e^{ik\mathcal{R}} A_{\ell, k}$ . The Fourier transformed equation becomes,

$$\partial_t A_{\ell, k} = 2J \sin(k) \left[ A_{\ell+1, k} - A_{\ell-1, k} \right] + \Gamma \left[ -2A_{\ell, k} + \delta_{\ell, 1} A_{-1, k} + \delta_{\ell, -1} A_{1, k} + 2 \cos(2k) \delta_{\ell, 0} A_{0, k} \right] \quad (\text{S46})$$

In the next section, we solve for the bound state of the above equation.

### E. Finite Noise Solution.

Our goal is to determine the ground state energy of the eigenvalue problem where we have parameterized the static hopping strength with  $J = \sin(\theta)$  and noise strength with  $\Gamma = \cos(\theta)$ ,

$$\mathcal{E}_q A_\ell = t_k(\theta) \left[ A_{\ell+1} - A_{\ell-1} \right] + \cos(\theta) \left[ -2A_\ell + \delta_{\ell, 1} A_{-1} + \delta_{\ell, -1} A_1 + 2 \cos(2k) \delta_{\ell, 0} A_0 \right]. \quad (\text{S47})$$

We have dropped the subscript  $k$  since we are solving these for a fixed momentum and  $t_k(\theta) = 2J \sin(k) \sin(\theta)$  is the effective hopping strength. For finite noise, the above equation is non-hermitian and effectively describes the dynamics of a one-dimensional hopping model. The above equation splits into four distinct eigenvalue equations,

$$\begin{aligned} \mathcal{E}_q A_0 &= t_k(\theta) (A_1 - A_{-1}) - 4 \cos(\theta) \sin^2(k) A_0 \\ \mathcal{E}_q A_1 &= t_k(\theta) (A_2 - A_0) - 2 \cos(\theta) A_1 + \cos(\theta) A_{-1} \\ \mathcal{E}_q A_{-1} &= t_k(\theta) (A_0 - A_{-2}) - 2 \cos(\theta) A_{-1} + \cos(\theta) A_1 \\ \mathcal{E}_q A_\ell &= t_k(\theta) (A_{\ell+1} - A_{\ell-1}) - 2 \cos(\theta) A_\ell, \end{aligned} \quad (\text{S48})$$

The final equation describes the bulk dynamics and sets the energy of the problem, while the first three equations are boundary conditions that constrain the allowed values that  $q$  can take. In the main text, we demonstrated that when

$\theta = 0$  the equation of motion for  $\ell = 0$  (which characterizes the correlation function) decouples from all other lengths, mapping onto a diffusion type equation. At this value, the above the eigenvalue equations are easily solved, and the entire spectrum is formed by horizontal lines at  $\mathcal{E} = -1, -2, -3$  where the fourth value is the diffusive mode  $-4k^2$  which is visualized in Fig. (S2)(c). We now attempt to solve for the diffusion constant for generic noise strength,  $\theta$ . First, we solve the bulk equation with the solution,  $A_\ell = Ae^{q\ell} + Be^{-q\ell+i\pi\ell}$ ,

$$\mathcal{E}_q = 4 \sin(k) \sinh(q) \sin(\theta) - 2 \cos(\theta) \quad (\text{S49})$$

Generically,  $q$  depends on momentum  $k$  which we determine through the equation  $A_0$ . First, if  $A_1$  and  $A_{-1}$  are known, then the entire set of coefficients is determined through the above equations; thus we use the ansatz,

$$A_\ell = \begin{cases} A_{-1}e^{q(1+\ell)} & \text{if } \ell \leq -1 \\ -A_1e^{q(1-\ell)+i\pi\ell} & \text{if } \ell \geq 1 \end{cases} \quad (\text{S50})$$

The three remaining equations solve for the variables  $A_1/A_{-1}$ ,  $A_0/A_{-1}$ , and  $q$ . The middle two equations solve for the ratios, and the equation for  $A_0$  restricts the values  $q$  takes. First, rewrite the middle two equations,

$$\left[ \mathcal{E}_q + 2e^{-q} \sin(k) \sin(\theta) + 2 \cos(\theta) \right] \frac{A_1}{A_{-1}} + 2 \sin(k) \sin(\theta) \frac{A_0}{A_{-1}} = \cos(\theta) \quad (\text{S51})$$

$$\left[ \mathcal{E}_q + 2e^{-q} \sin(k) \sin(\theta) + 2 \cos(\theta) \right] - 2 \sin(k) \sin(\theta) \frac{A_0}{A_{-1}} = \cos(\theta) \frac{A_1}{A_{-1}} \quad (\text{S52})$$

Solving these equations yields,

$$\frac{A_1}{A_{-1}} = -1, \quad \frac{A_0}{A_{-1}} = e^q + \frac{\cot(\theta)}{2 \sin(k)} \quad (\text{S53})$$

Here  $A_1$  and  $A_{-1}$  are determined through normalizing  $A_\ell$ . The value of  $A_0$  is determined through the second equation. The ratios above, combined with the final eigenvalue equation for  $A_0$  leads to the constraint,

$$\left[ \mathcal{E}_q + 4 \sin^2(k) \cos(\theta) \right] \left[ e^q + \frac{\cot(\theta)}{2 \sin(k)} \right] = -4 \sin(k) \sin(\theta) \quad (\text{S54})$$

The above equation is a cubic equation for  $q$ , which can be solved exactly. At small momentum, all three solutions to the cubic equation are physical and admit purely real energies; one corresponds to the largest real eigenvalue, the bound state energy. We solve the cubic equation and expand the bound state energy around  $k = 0$  giving  $q$ ,

$$e^q = \frac{\cot(\theta)}{k} - \frac{1}{6} [11 \cot(\theta) + 2 \tan(\theta)] k. \quad (\text{S55})$$

Inserting the above solution into the equation for the energy and keeping the lowest order in  $k$ , we find,

$$\mathcal{E}_q = 2k \sin(\theta) (e^q - e^{-q}) - 2 \cos(\theta) \approx -\frac{2}{3} [(5 + \cos(2\theta)) \sec(\theta)] k^2. \quad (\text{S56})$$

Moreover, regardless of the strength of the noisy hopping, the late-time hydrodynamic tail remains diffusive. In Fig. S2(c)-(f), we diagonalize Eq. (S47) for different noise strengths and plot the real part of the spectrum. For all strengths, the diffusive mode is present at small  $k$ , which we fit with the analytical result Eq. (S56) [see yellow curve]. As momentum increases, the bound state undergoes a phase transition by entering a continuum of scattering states at  $-2 \cos(\theta)$ , indicated by the red line in Fig. S2(c)-(f). Interestingly as  $k$  increases further, the bound state reemerges at an exceptional like point. At this point, the two physical solutions to the cubic equation, which give purely real energies, collide and become a pair of conjugate energies. Interestingly, there is a higher-order exceptional-like point near the strong noise limit where the solutions transition back to purely real non-degenerate energies; see Fig. S2(d). We also emphasize that an alternative solution to the above eigenvalue equations is to assume  $A_0 = 0$ , in which case you can determine analytically the form of the branch beginning at  $-\cos(\theta)$  in Fig. S2(c)-(f).

## F. Finite Noise Solution with Linear Potential.

We now reconsider the previous section, with a static linear potential. The general eigenvalue equation takes the form,

$$\mathcal{E}_q A_\ell = 2 \sin(\theta) \sin(k) \left[ A_{\ell+1} - A_{\ell-1} \right] + \cos(\theta) \left[ -2A_\ell + \delta_{\ell,1} A_{-1} + \delta_{\ell,-1} A_1 + 2 \cos(2k) \delta_{\ell,0} A_0 \right] + i\gamma \ell A_\ell. \quad (\text{S57})$$

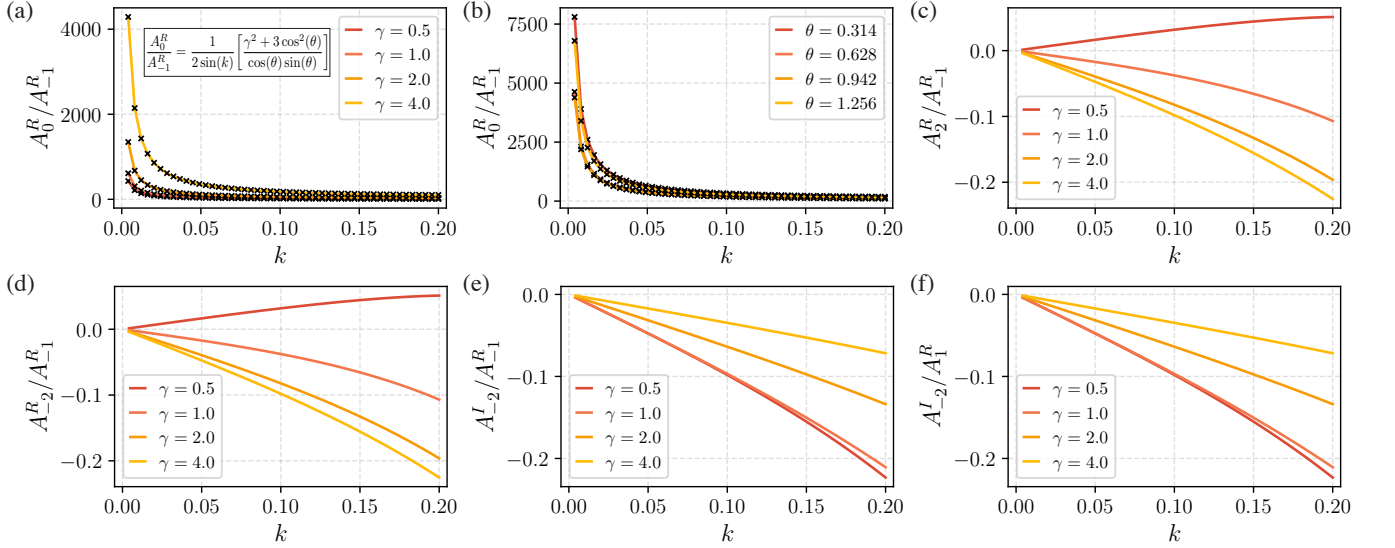


FIG. S3. *Coefficient Ratios for Linear Potential.* (a) Coefficient ratio  $A_0^R/A_{-1}^R$ , which governs the bound state energy scaling, as a function of momentum  $k$  for different potential strengths with  $\theta = \pi/4$ . The black crosses are from numerical diagonalization of Eq. (S57), while the curves are the analytical equation of the inset. (b) Same as (a) for  $\gamma = 4$  and different degrees of space-time translation breaking  $\theta$ . It is important to note that in both (a) and (b) the final points at  $k = 0.2$  are  $A_0^R/A_{-1}^R > 100$ . (c)  $A_2^R/A_{-1}^R$ , (d)  $A_{-2}^R/A_{-1}^R$ , (e)  $A_{-2}^I/A_{-1}^R$ , (f)  $A_{-2}^I/A_1^R$  for different potential strengths. To determine the analytical form of the bound state energy Eq. (S64) we neglected all  $A_{\pm 2}^R$  terms in the operator equations by arguing they are small compared to  $A_0^R/A_{-1}^R$ . These plots provide a numerical justification of this approximation, where clearly the ratios (c)-(f) are significantly smaller over the range of momentum and give a negligible contribution to the energy. Parameters:  $N = 400$

We note that with this potential the coordinate  $\mathcal{R}$  still has spatial translation invariance, however the explicit dependence on  $\ell$  prevents the ansatz used above. Moreover, we split Eq. (S57) into boundary and bulk equations,

$$\begin{aligned}
 \mathcal{E}_q A_0 &= t_k(\theta) (A_1 - A_{-1}) - 4 \cos(\theta) \sin^2(k) A_0 \\
 \mathcal{E}_q A_1 &= t_k(\theta) (A_2 - A_0) - 2 \cos(\theta) A_1 + \cos(\theta) A_{-1} + i\gamma A_1 \\
 \mathcal{E}_q A_{-1} &= t_k(\theta) (A_0 - A_{-2}) - 2 \cos(\theta) A_{-1} + \cos(\theta) A_1 - i\gamma A_{-1} \\
 \mathcal{E}_q A_\ell &= t_k(\theta) (A_{\ell+1} - A_{\ell-1}) - 2 \cos(\theta) A_\ell + i\gamma \ell A_\ell,
 \end{aligned} \tag{S58}$$

In the main text we re-scaled the energy  $\mathcal{E}_q \rightarrow \mathcal{E}_q(\theta) = \mathcal{E}_q + 2 \cos(\theta)$ . The bulk equation without the boundary conditions is anti-hermitian, therefore the energies are imaginary with a fixed real part, i.e.,  $\mathcal{E}_q = -2 \cos(\theta) + i\gamma q$  where  $q \in \{-\ell_{\max}, \ell_{\max}\}$ . In the noise free limit the energy becomes purely imaginary, forming a Wannier-Stark ladder leading non-thermal Bloch oscillations [see inset of Fig. 3(d) in the main text]. Including the boundary conditions  $A_0, A_1, A_{-1}$  at finite noise has the affect of turning the set of equations non-hermitian causing an eigenstate to emerge from the ladder with a purely real energy, which is the bound state that governs the hydrodynamic behavior. The bulk equation is the modified Bessel function recurrence relation, solve with the following,

$$A_\ell = \begin{cases} \mathcal{A}\mathcal{I}_{\nu_-}(-2it_k(\theta)/\gamma) & \text{if } \ell \leq -1 \\ \mathcal{B}\mathcal{I}_{\nu_+}(-2it_k(\theta)/\gamma) & \text{if } \ell \geq 1. \end{cases} \tag{S59}$$

where  $\mathcal{I}_{\nu_\pm}(iz)$  is the modified Bessel function of the first kind of order  $\nu_\pm = \frac{i\mathcal{E}_q(\theta)}{\gamma} \pm \ell$ . The difference in sign for the Bessel function order is to ensure that the solution decays to zero as  $\ell \rightarrow \pm\infty$ , otherwise it is generically a poorly behaved function on the left half.

### 1. Approximate solution to Bound State Energy.

Unlike the case without a potential, here determining the analytical form of the bound state energy is tricky because the solution to the recurrence relation explicitly depends on the energy through the Bessel function order. In the



previous section, determining the energy ultimately came down to finding a particular ratio of the coefficients. In this section, we construct a solution to the bound state energy by making a few approximations that make the calculation more tenable. To begin we expand the three equations for  $A_0$ , and  $A_{\pm 1}$  into six equations by breaking them into real and imaginary parts, i.e.,  $A_\ell = A_\ell^{\mathbb{R}} + iA_\ell^{\mathbb{I}}$ . The following set is as follows,

$$\begin{aligned}
\mathcal{E}_q A_0^{\mathbb{R}} &= t_k(\theta) (A_1^{\mathbb{R}} - A_{-1}^{\mathbb{R}}) - 4 \cos(\theta) \sin^2(k) A_0^{\mathbb{R}} \\
\mathcal{E}_q A_1^{\mathbb{R}} &= t_k(\theta) (A_2^{\mathbb{R}} - A_0^{\mathbb{R}}) - 2 \cos(\theta) A_1^{\mathbb{R}} + \cos(\theta) A_{-1}^{\mathbb{R}} - \gamma A_1^{\mathbb{I}} \\
\mathcal{E}_q A_{-1}^{\mathbb{R}} &= t_k(\theta) (A_0^{\mathbb{R}} - A_{-2}^{\mathbb{R}}) - 2 \cos(\theta) A_{-1}^{\mathbb{R}} + \cos(\theta) A_1^{\mathbb{R}} + \gamma A_{-1}^{\mathbb{I}} \\
\mathcal{E}_q A_0^{\mathbb{I}} &= t_k(\theta) (A_1^{\mathbb{I}} - A_{-1}^{\mathbb{I}}) - 4 \cos(\theta) \sin^2(k) A_0^{\mathbb{I}} \\
\mathcal{E}_q A_1^{\mathbb{I}} &= t_k(\theta) (A_2^{\mathbb{I}} - A_0^{\mathbb{I}}) - 2 \cos(\theta) A_1^{\mathbb{I}} + \cos(\theta) A_{-1}^{\mathbb{I}} + \gamma A_1^{\mathbb{R}} \\
\mathcal{E}_q A_{-1}^{\mathbb{I}} &= t_k(\theta) (A_0^{\mathbb{I}} - A_{-2}^{\mathbb{I}}) - 2 \cos(\theta) A_{-1}^{\mathbb{I}} + \cos(\theta) A_1^{\mathbb{I}} - \gamma A_{-1}^{\mathbb{R}}.
\end{aligned} \tag{S60}$$

From numerics we know the following features:  $A_1^{\mathbb{R}}/A_{-1}^{\mathbb{R}} = -1$ ,  $A_1^{\mathbb{I}}/A_{-1}^{\mathbb{I}} = 1$ , and  $A_0^{\mathbb{I}} = 0$ . Moreover, the bound state energy is solely determined by the ratio  $A_0^{\mathbb{R}}/A_{-1}^{\mathbb{R}}$ ,

$$\left[ \mathcal{E}_q + 4 \cos(\theta) \sin^2(k) \right] \frac{A_0^{\mathbb{R}}}{A_{-1}^{\mathbb{R}}} = -2t_k(\theta) \tag{S61}$$

To solve the above set of equations we first study the ratio  $A_0^{\mathbb{R}}/A_{-1}^{\mathbb{R}}$  as a function of momentum for different  $\gamma$  and  $\theta$  in Fig. S3(a) and (b) where the functional form roughly decays as  $\sim 1/k$ . We then numerically compare the ratios including  $A_{\pm 2}^{\mathbb{R}(\mathbb{I})}$  as a function of momentum in Fig. S3(c)-(f) and find that they are small compared to  $A_0^{\mathbb{R}}/A_{-1}^{\mathbb{R}}$  which has a final value greater than one-hundred. Moreover, in the equations above we set all  $A_{\pm 2}^{\mathbb{R}(\mathbb{I})} = 0$ . Next, we use the imaginary equations to determine the ratio  $A_1^{\mathbb{I}}/A_{-1}^{\mathbb{R}}$  and  $A_{-1}^{\mathbb{I}}/A_{-1}^{\mathbb{R}}$ , which we find to be,

$$\frac{A_{-1}^{\mathbb{I}}}{A_{-1}^{\mathbb{R}}} = \frac{-\gamma}{\mathcal{E}_q + \cos(\theta)}. \tag{S62}$$

Inserting this relation into the equations for  $A_1^{\mathbb{R}}, A_{-1}^{\mathbb{R}}$  we find that,

$$\frac{A_0^{\mathbb{R}}}{A_{-1}^{\mathbb{R}}} = \frac{\gamma^2 + \mathcal{E}_q^2 + 4\mathcal{E}_q \cos(\theta) + 3 \cos^2(\theta)}{2 \sin(k) \sin(\theta) (\mathcal{E}_q + \cos(\theta))} \approx \frac{\gamma^2 + 3 \cos^2(\theta)}{2 \sin(k) \cos(\theta) \sin(\theta)} \tag{S63}$$

Inserting into Eq. (S61) will give a cubic equation in  $\mathcal{E}_q$  just as in the previous section. Fig. S3(a) and (b) plot the above analytical result [solid curves] neglecting terms with  $\mathcal{E}_q$  and find perfect agreement with numerical diagonalization [black crosses]. With this approximation, we find the bound state energy has the scaling,

$$\mathcal{E}_q = -2 \cos(\theta) \sin^2(k) \left[ \frac{5 + 2\gamma^2 + \cos(2\theta)}{\gamma^2 + 3 \cos^2(\theta)} \right]. \tag{S64}$$

Note, the above result preserves the feature that when  $\theta = \pi/2$ ,  $\mathcal{E}_q = 0$  because there is not a bound state with a purely real energy, but rather an entire spectrum of bound states with purely complex energies that are equally spaced from the emergent Stark ladder. If instead we take the limit,  $\gamma = 0$  we recover the bound state energy for finite noise. We point out that in this case when momentum increases, the diffusive bound state does not meet a continuum of scattering states, but rather other bound states from the localization. It is then interesting that these bound states do not seem to appear in the correlation function, indicating that the ground state we found is significantly more dominant.

### G. Numerical Methods for Determining the Coefficients.

We now outline how in the main text we numerically determined the two-point correlation function from the coefficient,  $A_{\ell,k}$ . First, we put an upper limit on the operator length labelled  $\ell_{\max}$  such that,

$$\vec{A} = (A_{-\ell_{\max},k}, \dots, A_{0,k}, \dots, A_{\ell_{\max},k}). \tag{S65}$$

The above vector obeys the matrix differential equation,

$$\frac{d\vec{A}(t)}{dt} = M\vec{A}(t) \quad (\text{S66})$$

where the matrix  $M$  is determined from Eq. (10) in the main text which is diagonalized as  $M = VDV^{-1}$  where  $V$  is set of eigenvectors and  $D = \text{diag}(\lambda_1, \dots, \lambda_{2\ell_{\max}+1})$ . Upon making the above change of basis the differential equation above becomes,

$$\frac{d\vec{\Sigma}(t)}{dt} = D\vec{\Sigma}(t). \quad (\text{S67})$$

Here  $\vec{\Sigma} = V^{-1}\vec{A}$  and the equation is easily integrated to give,  $\vec{\Sigma}(t) = e^{Dt}\vec{\Sigma}(0)$ . Mapping back to the original basis, the coefficients are found to be,

$$\vec{A}(t) = (Ve^{Dt}V^{-1})\vec{A}(0). \quad (\text{S68})$$

We then extract the element  $[\vec{A}(t)]_{0,k}$  for each momentum and then perform the following sum,

$$C_{x,y}(t) = \frac{1}{8\pi} \sum_k [\vec{A}(t)]_{0,k} e^{i(x-y)k}. \quad (\text{S69})$$

## S5. TIME-DEPENDENT POTENTIAL.

In this section, from the noise-averaged operator equation of motion, we derive the differential equations for the coefficients in the operator expansion. Here we focus on the case where the hopping is static and nearest-neighbor which corresponds to  $J_{x,x} = 0$ ,  $J_{x,x+1} = J$  and the noise is coupled to the density, i.e.,  $\Gamma_{x,x+1} = 0$ . We begin by first deriving the contribution from the incoherent term as the coherent piece is the same as above.

### A. Incoherent Term

In this section, we derive the incoherent piece that arises from the variance of the couplings,

$$\sum_x \mathcal{L}_x[\bar{n}_t] = \sum_x \sum_{m,n} A_{m,n} \left[ n_x c_m^\dagger c_n n_x - \frac{1}{2} \{n_x, c_m^\dagger c_n\} \right]. \quad (\text{S70})$$

As in the previous section, the final result must be a product of two fermionic operators. We first calculate the second term in the above equation,

$$\begin{aligned} \{n_x, c_m^\dagger c_n\} &= c_x^\dagger c_x c_m^\dagger c_n + c_m^\dagger c_n c_x^\dagger c_x \\ &= c_x^\dagger (\delta_{m,x} - c_m^\dagger c_x) c_n + c_m^\dagger (\delta_{x,n} - c_x^\dagger c_n) c_x \\ &= \delta_{m,x} c_x^\dagger c_n + c_m^\dagger c_x^\dagger c_x c_n + c_m^\dagger c_x^\dagger c_x c_n + \delta_{n,x} c_m^\dagger c_x \\ &= 2c_m^\dagger c_x^\dagger c_x c_n + \delta_{m,x} c_x^\dagger c_n + \delta_{n,x} c_m^\dagger c_x. \end{aligned} \quad (\text{S71})$$

We put the fermion operators in normal order to simplify all these expressions. Therefore, in the first equation above, we use the anti-commutator to move the creation operators to the left and then do algebra on the subsequent lines. Combing everything, we have that,

$$-\frac{1}{2} \{n_x, \bar{n}_t\} = -\sum_x \sum_{m,n} A_{m,n} c_m^\dagger c_x^\dagger c_x c_n - \sum_{mn} A_{m,n} c_m^\dagger c_n. \quad (\text{S72})$$

We resolved the delta functions in the second term to eliminate the sum over  $x$ . Note that if  $A_{m,n} = \delta_{x,m} \delta_{x,n}$  we get that the above equation is  $-n_x$  which we expect from  $-\frac{1}{2} \{n_x, n_x\} = -n_x$ . Another check is if  $A_{m,n} = \delta_{y,m} \delta_{y,n}$  then we find  $-n_y n_x$  as expected. We now compute the first term, which is a product of six fermion operators,

$$\begin{aligned} c_x^\dagger c_x c_m^\dagger c_n c_x^\dagger c_x &= c_x^\dagger (\delta_{m,x} - c_m^\dagger c_x) c_n c_x^\dagger c_x \\ &= \delta_{m,x} c_x^\dagger c_n c_x^\dagger c_x - c_x^\dagger c_m^\dagger c_x c_n c_x^\dagger c_x \\ &= \delta_{m,x} c_x^\dagger c_n c_x^\dagger c_x - \delta_{n,x} c_x^\dagger c_m^\dagger c_x c_n c_x + c_x^\dagger c_m^\dagger c_x c_x^\dagger c_n c_x \\ &= \delta_{m,x} c_x^\dagger c_n c_x^\dagger c_x + c_x^\dagger c_m^\dagger c_n c_x \end{aligned} \quad (\text{S73})$$

In total we have that,

$$\sum_x \sum_{m,n} A_{m,n} c_x^\dagger c_x c_m^\dagger c_n c_x^\dagger c_x = \sum_x \sum_{m,n} A_{m,n} \left[ \delta_{m,x} c_x^\dagger c_n c_x^\dagger c_x + c_x^\dagger c_m^\dagger c_n c_x \right] \quad (\text{S74})$$

We now combine the previous two results,

$$\begin{aligned} \sum_x \mathcal{L}_x [\bar{n}_t] &= \sum_x \sum_{m,n} A_{m,n} c_x^\dagger c_x c_m^\dagger c_n c_x^\dagger c_x - \frac{1}{2} A_{m,n} \{n_x, c_m^\dagger c_n\} \\ &= \sum_x \sum_{m,n} A_{m,n} \left[ \delta_{m,x} c_x^\dagger c_n c_x^\dagger c_x + c_x^\dagger c_m^\dagger c_n c_x \right] - \sum_x \sum_{m,n} A_{m,n} c_m^\dagger c_x^\dagger c_x c_n - \sum_{m,n} A_{m,n} c_m^\dagger c_n \\ &= \sum_x \sum_{m,n} A_{m,n} \delta_{m,x} c_x^\dagger c_n c_x^\dagger c_x - \sum_{m,n} A_{m,n} c_m^\dagger c_n \\ &= \sum_{m,n} A_{m,n} c_m^\dagger c_n c_m^\dagger c_m - \sum_{m,n} A_{m,n} c_m^\dagger c_n \end{aligned} \quad (\text{S75})$$

There are a few checks we can perform on the above equation. First, if  $A_{m,n} = \delta_{x,m} \delta_{x,n}$  or  $A_{m,n} = \delta_{y,m} \delta_{y,n}$  the above result vanishes. When the Lindblad acts on a number operator, i.e.,  $\mathcal{L}[c_\alpha^\dagger c_\alpha]$ , it annihilates it. The final simplification is the normal ordering of the first term above,

$$\sum_x \mathcal{L}_x [\bar{n}_t] = \sum_{m,n} A_{m,n} (\delta_{n,m} c_m^\dagger c_m - c_m^\dagger c_n) \quad (\text{S76})$$

Notice above that if the operator is on the same site, i.e.,  $m = n$ , then we get zero, and if  $m \neq n$ , we get  $-\bar{n}_t$ . Thus we can rewrite the above equation as,

$$\sum_x \mathcal{L}_x [\bar{n}_t] = \sum_{mn} A_{m,n} (\delta_{nm} - 1) c_m^\dagger c_n \quad (\text{S77})$$

Moreover, the final differential equation becomes,

$$\frac{d\bar{n}_t}{dt} = \frac{dA_{m,n}}{dt} = iJ[A_{m+1,n} - A_{m,n-1} + A_{m-1,n} - A_{m,n+1}] + \Gamma A_{m,n} (\delta_{nm} - 1) \quad (\text{S78})$$

## B. Mapping to $\ell$ and $\mathcal{R}$

In this section, we rewrite the final equation of the previous section in a different coordinate system defined by the variables  $\ell = n - m$  and  $\mathcal{R} = n + m$ . Here  $\ell$  represents the length of the operator, and  $\mathcal{R}$  is the center of mass of the operator. The coefficients under this mapping become,

$$\begin{aligned} A_{m+1,n} &\xrightarrow{(n-m-1=\ell-1, n+m+1=\mathcal{R}+1)} A_{\ell-1, \mathcal{R}+1}, & A_{m,n-1} &\xrightarrow{(n-1-m=\ell-1, n-1+m=\mathcal{R}-1)} A_{\ell-1, \mathcal{R}-1} \\ A_{m-1,n} &\xrightarrow{(n-m+1=\ell+1, n+m-1=\mathcal{R}-1)} A_{\ell+1, \mathcal{R}-1}, & A_{m,n+1} &\xrightarrow{(n+1-m=\ell+1, n+1+m=\mathcal{R}+1)} A_{\ell+1, \mathcal{R}+1} \\ A_{m,n} &\xrightarrow{(n-m=\ell, n+m=\mathcal{R})} A_{\ell, \mathcal{R}}, & \delta_{m,n} &\xrightarrow{(n-m=0)} \delta_{\ell,0}. \end{aligned} \quad (\text{S79})$$

Moreover, the differential equation becomes,

$$\frac{dA_{\ell, \mathcal{R}}}{dt} = iJ[A_{\ell-1, \mathcal{R}+1} - A_{\ell+1, \mathcal{R}+1} + A_{\ell+1, \mathcal{R}-1} - A_{\ell-1, \mathcal{R}-1}] + \Gamma A_{\ell, \mathcal{R}} (\delta_{\ell,0} - 1) \quad (\text{S80})$$

The advantage of moving into this coordinate system is that the delta function is independent of  $R$ ; thus, we can perform a discrete Fourier transformation  $A_{\ell, \mathcal{R}} = \sum_k e^{ik\mathcal{R}} A_{\ell, k}$  where  $k$  is the momentum of the Brillouin zone. The Fourier transformed equation becomes,

$$\frac{dA_{\ell, k}}{dt} = t_k [A_{\ell+1, k} - A_{\ell-1, k}] + \Gamma A_{\ell, k} (\delta_{\ell,0} - 1). \quad (\text{S81})$$

This equation describes an effective model where a particle hops in one dimension with hopping strength  $t_k = 2J \sin(k)$  with a delta function at the center of the chain. The above equation is a matrix differential equation where the ground state is given by the bound state of the delta function and ultimately determines the late-time hydrodynamic response.

### C. Solving Ground State Eigenvalue Problem

Our goal is to determine the ground state of the eigenvalue equation ( $\Gamma = 1$ ),

$$\mathcal{E}_q A_{\ell,k} = t_k (A_{\ell+1,k} - A_{\ell-1,k}) + (\delta_{\ell,0} - 1) A_{\ell,k} \quad (\text{S82})$$

We now split the above equation into two different equations,

$$\mathcal{E}_q A_{0,k} = t_k (A_{1,k} - A_{-1,k}) \quad (\text{S83})$$

$$\mathcal{E}_q A_{\ell,k} = t_k (A_{\ell+1,k} - A_{\ell-1,k}) - A_{\ell,k}, \quad (\text{S84})$$

where  $\ell$  represents the entire line without zero. Using the second equation, we can determine the energy by assuming the ansatz,  $A_\ell = Ae^{q\ell} + Be^{-q\ell+i\pi\ell}$  leading to the relation,

$$(1 + \mathcal{E}_q) (Ae^{q\ell} + Be^{-q\ell+i\pi\ell}) = 2J \sin(k) \left[ Ae^{q\ell} (e^{-q} - e^q) + Be^{-q\ell+i\pi\ell} (e^{q+i\pi} - e^{-q+i\pi}) \right] \quad (\text{S85})$$

$$= 4J \sin(k) \sinh(q) (Ae^{q\ell} + Be^{-q\ell+i\pi\ell}). \quad (\text{S86})$$

Moreover, the energy is determined as

$$\mathcal{E}_q = 4J \sin(k) \sinh(q) - 1 \quad (\text{S87})$$

The next step is to determine the values  $q$  can take. First, we write the solution to the second equation in both regions,

$$A_\ell = \begin{cases} Ae^{q\ell} + Be^{-q\ell+i\pi\ell} & \text{if } \ell < 0 \\ Ce^{q\ell} + De^{-q\ell+i\pi\ell} & \text{if } \ell > 0 \end{cases} \quad (\text{S88})$$

In the region  $\ell \leq 0$  the second term is unbounded as  $\ell \rightarrow -\infty$  thereby we set  $B = 0$ . Similarly, for  $\ell \geq 0$  the first term is unbounded as  $\ell \rightarrow \infty$  and we therefore also set  $C = 0$ . A further constraint is made at  $\ell = 0$  which sets  $A = D$  and the general solution becomes,

$$A_\ell = \begin{cases} Ae^{q\ell} & \text{if } \ell \leq 0 \\ Ae^{-q\ell+i\pi\ell} & \text{if } \ell \geq 0. \end{cases} \quad (\text{S89})$$

With this solution, we can determine  $A_1$  and  $A_{-1}$  and inset them into the first equation above for  $A_0$  which leads to the constraint on  $q$ ,

$$\begin{aligned} \mathcal{E}_q A &= 2J \sin(k) [-Ae^{-q} - Ae^{-q}] \\ &= -4J \sin(k) e^{-q} \\ &= 4J \sin(k) \sinh(q) - 1 \end{aligned} \quad (\text{S90})$$

From this, we find that  $q$  is

$$q = \cosh^{-1} \left[ \frac{1}{4J \sin(k)} \right] \quad (\text{S91})$$

If now assume to be near the bottom of the band such that  $\sin(k) \approx k$  then we find the energy as follows,

$$\mathcal{E}_q = 4Jk \left[ \frac{\sqrt{1 - 16J^2 k^2}}{4Jk} \right] - 1 \approx -8J^2 k^k \quad (\text{S92})$$

Where because  $k$  is small we binomially expand the square root and find that the bound state energy scales as  $k^2$  which indicates diffusion at late times.